







New insights into cholesterol-mediated $ERR\alpha$ activation in breast cancer progression and pro-tumoral microenvironment orchestration

Matteo Brindisi^{1,2} , Luca Frattaruolo¹, Marco Fiorillo^{1,3} , Vincenza Dolce¹ ,
Federica Sotgia² , Michael P. Lisanti²  and Anna Rita Cappello¹ 

1 Department of Pharmacy, Health and Nutritional Sciences, University of Calabria, Rende, Italy

2 Cell Adhesion Unit, Vita-Salute San Raffaele University, Milan, Italy

3 Translational Medicine, School of Science, Engineering and the Environment (SEE), University of Salford, Manchester, UK

Keywords

cancer aggressiveness; cholesterol; EMT; $ERR\alpha$; tumour microenvironment

Correspondence

F. Sotgia and M. P. Lisanti, Cell Adhesion Unit, Vita-Salute San Raffaele University, Via Olgettina, Milan (MI), Italy

Tel: +Xxxxx

E-mails: f.sotgia@salford.ac.uk (FS);

m.p.lisanti@salford.ac.uk (MPL)

and

A. R. Cappello, Department of Pharmacy, Health and Nutritional Sciences, University of Calabria, Via P. Bucci, 87036 Rende (CS), Italy

Tel: +Xxxxx

E-mail: annarita.cappello@unical.it

Matteo Brindisi and Luca Frattaruolo contributed equally to this article

(Received 27 December 2021, revised 8 September 2022, accepted 12 October 2022)

doi:10.1111/febs.16651

Introduction


The exact mechanisms underlying the onset, development and progression of breast cancer remain poorly

Breast cancer remains the greatest cause of cancer-related death in women worldwide. Its aggressiveness and progression derive from intricate processes that occur simultaneously both within the tumour itself and in the neighbouring cells that make up its microenvironment. The aim of the present work was firstly to study how elevated cholesterol levels increase tumour aggressiveness. Herein, we demonstrate that cholesterol, by activating $ERR\alpha$ pathway, promotes epithelium-mesenchymal transition (EMT) in breast cancer cells (MCF-7 and MDA-MB-231) as well as the release of pro-inflammatory factors able to orchestrate the tumour microenvironment. A further objective of this work was to study the close symbiosis between tumour cells and the microenvironment. Our results allow us to highlight, for the first time, that breast cancer cells exposed to high cholesterol levels promote (a) greater macrophages infiltration with induction of an M2 phenotype, (b) angiogenesis and endothelial branching, as well as (c) a cancer-associated fibroblasts (CAFs) phenotype. The effects observed could be due to direct activation of the $ERR\alpha$ pathway by high cholesterol levels, since the simultaneous inhibition of this pathway subverts such effects. Overall, these findings enable us to identify the cholesterol- $ERR\alpha$ synergy as an interesting target for breast cancer treatment.

understood. In fact, there are several signalling pathways that contribute to these processes [1–3]. Within

Abbreviations

CAF, cancer-associated fibroblast; CD163, haemoglobin scavenger receptor; EMT, epithelium-mesenchymal transition; $ERR\alpha$, oestrogen-related receptor α ; $ER\alpha$, oestrogen receptor alpha; FAP, fibroblast activation protein; HMGCR, 3-hydroxy-3-methyl-glutaryl-coenzyme A reductase; IL, interleukin; LPS, lipopolysaccharide; MMP-9, Matrix metalloproteinase-9; PMA, Phorbol 12-myristate 13-acetate; qPCR, quantitative polymerase chain reaction; ROS, reactive oxygen species; TAM, tumour-associated macrophages; TGF- β , transforming growth factor- β ; TME, tumour microenvironment; TNF α , tumour necrosis factor- α ; ZEB-1, Zinc finger E-box-binding homeobox 1; α -SMA, α -smooth muscle actin.

Dispatch: 22.10.22	CE: Geetha M
No. of pages: 21	PE: Maheswari M.
WILEY	
16651 / FJ-21-1247.R2	Manuscript No.
FEBS	Journal Code
	

1 them, of note there are nuclear receptors which act as
2 transcription factors by regulating the expression of
3 specific genes involved in pathophysiological processes
4 [4–6]. In particular, we focused our attention on
5 oestrogen-related receptor alpha (ERR α), an orphan
6 nuclear receptor, without a natural ligand *in vivo*.
7 Cholesterol was recently identified by Wei et al. [7] as
8 an endogenous ligand, acting as a agonist to this
9 receptor. ERR α is structurally related to ER α , but the
10 typical ligands of the latter, such as 17- β -oestradiol,
11 are unable to activate it as the ligand binding site is
12 different. ERR α 's transcriptional activity immediately
13 attracted considerable attention in the research world
14 [8–12]. In fact, since the first identification of ERR α , a
15 growing number of reports have described its function
16 in important physiological and metabolic processes
17 such as bone homeostasis or autophagy [13–15]. At
18 the same time, in recent years, there have been many
19 reports in which the ERR α signalling pathway is asso-
20 ciated with important pathological processes such as
21 tumorigenesis [16,17], as ERR α expression has been
22 found to be dysregulated in colon, endometrial, pros-
23 tate, ovarian and breast carcinoma, while its levels are
24 negatively correlated with patient survival [18–20].

25 Recently, we demonstrated that high cholesterol
26 concentrations increase ERR α expression levels with
27 further activation of a dense signalling network able to
28 induce greater development and progression of breast
29 cancer regardless of molecular subtype [21]. Further-
30 more, the activation of the ERR α signalling network
31 was found to be related to metabolic switches which
32 can cope with both the considerable metabolic require-
33 ment needed to sustain the marked neoplastic prolifer-
34 ation and progression, typical of cancer and the
35 noticeable production of lipid droplets [21]. Taken
36 together, these features confer greater resistance to the
37 normal therapeutic regimens currently used for breast
38 cancer treatment [21].

39 However, the mechanisms underlying neoplastic
40 development and progression are not limited only to
41 cancer cells but also extend to the environment sur-
42 rounding the tumour, the so-called tumour microenvi-
43 ronment (TME) [22,23]. Since the seed and soil theory
44 was proposed by Paget a century ago [24,25], research
45 has led to a significant increase in our knowledge of
46 the tumour 'seed,' but little is still known about the
47 'soil,' that is the microenvironment, the stromal cells
48 surrounding the tumour, in particular with regard to
49 the exact mechanisms by which once it has been
50 affected by cancer cells, the microenvironment pro-
51 motes their progression.

52 There are numerous reports describing the close
53 symbiosis that is created between tumour cells and the

microenvironment [25,26]; indeed, the tumour exploits
this, thus ensuring greater cancer cell progression, as
well as their increased ability to disseminate through-
out the body. Macrophages, endothelial cells and
fibroblasts are the main microenvironment compo-
nents, which are found to actively collaborate with
tumour cells [27,28].

In this regard, once tumour-associated macrophages
(TAMs) are affected by factors released by the
tumour, they induce a pro-tumorigenic inflammation,
subverting the healthy cells that make up the neigh-
bouring tissue [29]. On the other hand, endothelial cell
activation causes strong intratumoral angiogenesis,
giving the tumour itself an advantage in terms both of
development, through the intake of oxygen and nutri-
ents, and dissemination, due to the entry of cancer
cells into the bloodstream [30]. Acting as a 'glue'
between the two cell types are cancer-associated
fibroblasts (CAFs). They are the major stromal com-
ponent surrounding the tumour, providing it not only
with mechanical support but controlling and coordi-
nating all the other above-mentioned tumour microen-
vironment cells, in order to promote neoplastic
progression [31,32].

Therefore, the study of the metabolic reprogram-
ming of cancer cells cannot disregard the close symbio-
sis between the microenvironment and the tumour in
order to better characterize the phenotype and identify
new and efficient therapeutic targets.

It is precisely by examining the symbiosis between
breast cancer and its microenvironment that in the
present work we sought to unmask how, by activating
the ERR α pathway, high cholesterol levels promote
breast cancer progression. To this purpose, we aimed
both to evaluate whether ERR α pathway activation,
mediated by high cholesterol levels, could induce
epithelial-mesenchymal transition (EMT) in breast can-
cer cells and to assess whether these cells were able to
create a microenvironment that could promote their
progression.

The main goal was to establish that the ERR α sig-
nalling network should be assumed to be a key target
in breast cancer treatment.

Results

Cholesterol contributes to the EMT induction

The effects of high cholesterol levels in promoting
epithelial-mesenchymal transition (EMT) in breast can-
cer cells were evaluated using real-time PCR assay and
immunoblot analysis. Treatment of MCF-7 (ER α +) and
MDA-MB-231 (triple negative) breast cancer cells

with 10 μM cholesterol, a concentration able to activate $\text{ERR}\alpha$ as previously reported [21,33,34], showed that several markers typical of the EMT-associated pathway were over-expressed (Fig. 1).

The markers were evaluated at the transcriptional level, by quantifying the mRNA levels through qPCR experiments, as well as at the translational level by evaluating the protein expression levels with immunoblot assay. In detail, the MCF-7 cells treated with cholesterol showed a marked increase in the expression levels of vimentin, two-fold compared to the control, matrix metalloproteinases-9 (MMP-9), about 8-fold compared to the control, Zinc finger E-box binding homeobox 1 (ZEB-1), two times with respect to control and a slight reduction of E-cadherin levels, at a translational and transcriptional level (Fig. 1 panels A, D). Similar results were observed in MDA-MB-231 cells, with an increase in the expression levels of vimentin, three times with respect to control, matrix metalloproteinases-9 (MMP-9), two-fold compared to the control, Zinc finger E-box binding homeobox 1 (ZEB-1), about two-fold compared to the control and a slight reduction of E-cadherin expression observed just at transcriptional level, since E-cadherin, a protein already very poorly expressed in this cell line, was not detectable at translational level. In order to quantify the secretion levels and activity of MMP-9, the culture media of the tumour cells treated or not with cholesterol was used for the zymography assay (Fig. 1 panel F). Moreover, given the MCF-7 cells' poor ability to release MMP-9 into the culture media, in order to ensure an appreciable basal expression level thereof, the cells were simultaneously treated with phorbol 12-myristate 13-acetate (PMA), which is known to increase secretion of matrix metalloproteinase-9. Both cell lines showed that MMP-9 secretion in the culture media of cells treated with cholesterol was higher about 1.5-fold than in the respective baseline controls. Based on these results and in order to ascribe the ability to activate EMT processes to the cholesterol- $\text{ERR}\alpha$ synergy, we used 5 μM XCT-790, a known $\text{ERR}\alpha$ inverse agonist. To this end, breast cancer cells were treated with cholesterol in the presence of XCT-790 in order to inhibit the signalling induced by $\text{ERR}\alpha$. The results (Fig. 1 panel A) highlighted that vimentin and E-cadherin levels remain stable after cholesterol and XCT-790 co-treatment, confirming dependence on the $\text{ERR}\alpha$ pathway. Conversely, expression levels of ZEB-1 and MMP-9, albeit to a lesser extent, also increase in the presence of XCT-790 (Fig. 1), highlighting that some effects mediated by cholesterol in perturbing EMT-related pathways may be independent from the $\text{ERR}\alpha$ pathway. XCT-790 is widely used to inhibit

$\text{ERR}\alpha$ signalling, but it is also associated with other off-target effects such as inhibition of mitochondrial energy production [35]. On this basis, we checked the effects of cholesterol on MCF-7 cells silenced for ESSRA coding for $\text{ERR}\alpha$, in order to confirm cholesterol effects and to validate the use of XCT-790 as an $\text{ERR}\alpha$ inhibitor in our conditions. Firstly, $\text{ERR}\alpha$ expression levels in two different clones of MCF-7 sh $\text{ERR}\alpha$ were checked by immunoblot analysis (Fig. 1B), in order to choose for the subsequent experiments the clone that properly featured $\text{ERR}\alpha$ suppression. Then, as performed above, mRNA levels of EMT markers were evaluated by qPCR experiments. In detail, MCF-7 sh $\text{ERR}\alpha$ cells treated with cholesterol showed stable levels of all EMT markers, with a slight but not significant increasing trend in MMP-9 and ZEB-1 expression levels (Fig. 1C), thus confirming the outcomes obtained after XCT-790 treatment.

Cholesterol promotes pro-inflammatory factors secretion in breast cancer cells, by activating $\text{ERR}\alpha$ pathway

Tumour cells, in order to promote their progression, release several soluble factors able to promote pro-tumour microenvironment creation into the surrounding environment [36,37]. To this end, the levels of a large panel of cytokines and soluble factors released into the culture media by the cholesterol-treated breast cancer cells were evaluated using the cytokine array. The results, presented in Fig. 2, evidenced that the treatment of $\text{ER}\alpha$ + breast cancer cells with 10 μM cholesterol for 48 h significantly increases the release of Eotaxin-1 as well as IL-1 β , IL-2, IL-3, IL-6 and IL-7, with an increase ranging from two- to seven-fold (IL-6) with respect to the control. Similarly, treatment of the triple-negative breast cancer cell line showed enhanced levels of Eotaxin-2, IL-1 β , IL-3, IL-4, IL-6, IL-11 and IL-12 (p40 and p70 portions), about two-fold with respect to the control. Besides, the levels of all these pro-inflammatory mediators remained stable (except for a slight increase in Eotaxin-2 level in MCF-7 cells) after concomitant treatment of breast cancer cells with XCT-790 and cholesterol with respect to cells treated with XCT-790 alone. (Fig. 2 panels B,D).

Cholesterol promotes M2 polarization and macrophages chemotaxis, by activating $\text{ERR}\alpha$ pathway

Having highlighted cholesterol's effects in mediating the release of pro-inflammatory factors by breast cancer cells, we next asked whether and how macrophages were affected by conditioned media, obtained from breast

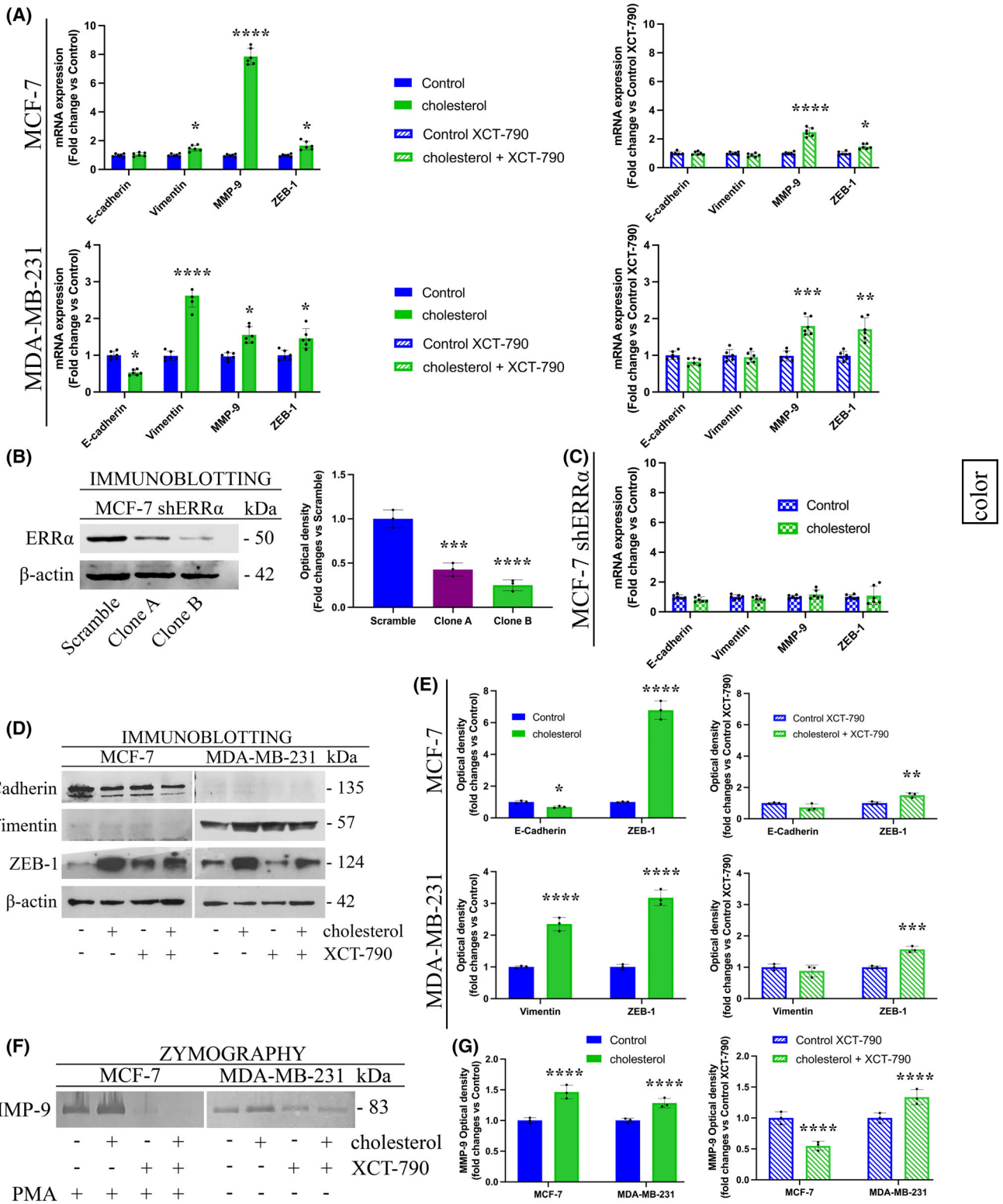


Fig. 1. High cholesterol levels promote the epithelial-mesenchymal transition process. (A) Real-time analysis of EMT markers in MCF-7 and MDA-MB-231 cells treated with EtOH (Control), 5 μM XCT-790 (Control XCT-790), 10 μM cholesterol or co-treated with 10 μM cholesterol and 5 μM XCT-790, for 48 h ($n = 6$). (B) Immunoblot analysis and respective optical density of MCF-7 shERR α clones. (C) Real-time analysis of EMT markers in MCF-7 shERR α cells treated with EtOH (Control) or 10 μM cholesterol for 48 h ($n = 3$). (D) Immunoblot analysis and respective optical density (E) of EMT markers in MCF-7 and MDA-MB-231 cells treated with EtOH (Control), 5 μM XCT-790 (Control XCT-790), 10 μM cholesterol or co-treated with 10 μM cholesterol and 5 μM XCT-790, for 48 h ($n = 3$). (F) Gel-zymography experiment and respective optical density (G) of MMP-9 in MCF-7 and MDA-MB-231 cells treated with EtOH (Control), 5 μM XCT-790 (Control XCT-790), 10 μM cholesterol or co-treated with 10 μM cholesterol and 5 μM XCT-790, for 48 h ($n = 3$). To ensure appreciable levels of MMP-9, MCF-7 cells were previously exposed to PMA. Values represent the mean \pm SD of three independent experiments. Statistical analysis was performed using Student's *t*-test (A, C, E, G) or One-way ANOVA analysis (B). **P*-value < 0.05; ***P*-value < 0.01; ****P*-value < 0.001; *****P*-value < 0.0001.

cancer cells treated with 10 μM cholesterol for 48 h. Macrophages are one of the main cell lines involved in setting up the microenvironment [38–40]. For this purpose, first of all, the THP-1 monocyte cell line was treated with 100 nM PMA in order to induce M0 polarization (tissue macrophages). The day after PMA treatment, macrophages were cultured in fresh media and then, the next day, treated with 10 ng·mL⁻¹ LPS or 20 ng·mL⁻¹ IL-4, in order to polarize them into the M1 or M2 state, respectively. As shown in Fig. 3 (panels A, B), the different polarization stages were evaluated by assessing the mRNA levels of different markers that characterize macrophage activation, such as IL-6, TNF α , CD163 and IL-10 and by morphological analysis using May-Grünwald-Giemsa staining [41].

The results highlight different transcriptional levels of tested cytokines as well as clear morphological differences between the polarization stages (Fig. 3 panel B). IL-6 and TNF- α expression were found to be very high in the M1 stage (thousand- and hundred-fold, respectively, compared to M0 stage), while CD163 and IL-10 stood out in the M2 stage (ten- and two-fold, respectively, compared to M0 stage; Fig. 3 panel A), thus defining these markers as representative of stages M1 and M2, respectively, in accordance with literature data [42]. Next, THP-1 cells polarized in the M0 stage were treated with the media from untreated breast cancer cells revealing their ability to promote heterogeneous macrophage activation characterized by a mixed M1 and M2 population (Fig. 3 panel C,D), as already highlighted in the literature data [43].

Based on that, we treated THP-1 cells polarized in the M0 stage with conditioned media from breast cancer cells exposed to 10 μM cholesterol for 48 h, in order to investigate the role of cholesterol in macrophage activation.

After treatment with conditioned media from MCF-7 and MDA-MB-231 cells previously exposed to cholesterol, macrophages experienced transcriptional increases of CD163 and IL-10, two markers which characterize the M2 pro-tumour macrophages (Fig. 4 panels A,D, respectively). Furthermore, the

morphological analysis highlighted slight changes typical of M2 polarization (Fig. 4 panel C,F). Besides, the culture media from MCF-7 and MDA-MB-231 cells simultaneously treated with cholesterol and XCT-790 did not induce an increase in M2 markers, by contrast with what was observed with the media derived from MCF-7 and MDA-MB-231 exposed to cholesterol alone (Fig. 4 panels B,E, respectively). Since macrophage activation could be related to mitochondrial activity impairments [44,45], also in this case, the results obtained after XCT-790 treatment were confirmed in MCF-7 shERR α , in order to exclude any off-target effects of XCT-790. As shown in Fig. 4 panel G, we treated THP-1 cells polarized in the M0 stage with conditioned media from MCF-7 shERR α previously exposed to 10 μM cholesterol for 48 h. In this condition, cholesterol treatment was not able to induce any increase in M2 markers, exactly as observed following XCT-790 co-treatment.

The evident M2 activation, induced by the culture media from tumour cells exposed to cholesterol treatment, prompted us to perform the cell migration assay, in order to evaluate whether the media from the treated tumour cells was able to exert a chemotactic effect on monocytes. To evaluate this, the THP-1 cells were seeded in the upper part of the polycarbonate septa with 8 μm pores, while the culture media from MCF-7 and MDA-MB-231 cells exposed or not to 10 μM cholesterol for 48 h was placed in the lower part and left to incubate for 6 h.

The results, shown in Fig. 5, revealed that the culture media from the cells exposed to cholesterol was able to induce a strong chemotactic effect, as evidenced by the higher number of THP-1 cells capable of invading the septum (1.5-fold for MCF-7 and 3-fold for MDA-MB-231), compared to their controls (THP-1 cells cultured in media from untreated breast cancer cells). Furthermore, even in this case, the culture media from MCF-7 and MDA-MB-231 cells simultaneously treated with cholesterol and XCT-790 did not induce an increase in the chemotactic effect highlighted by cholesterol alone.

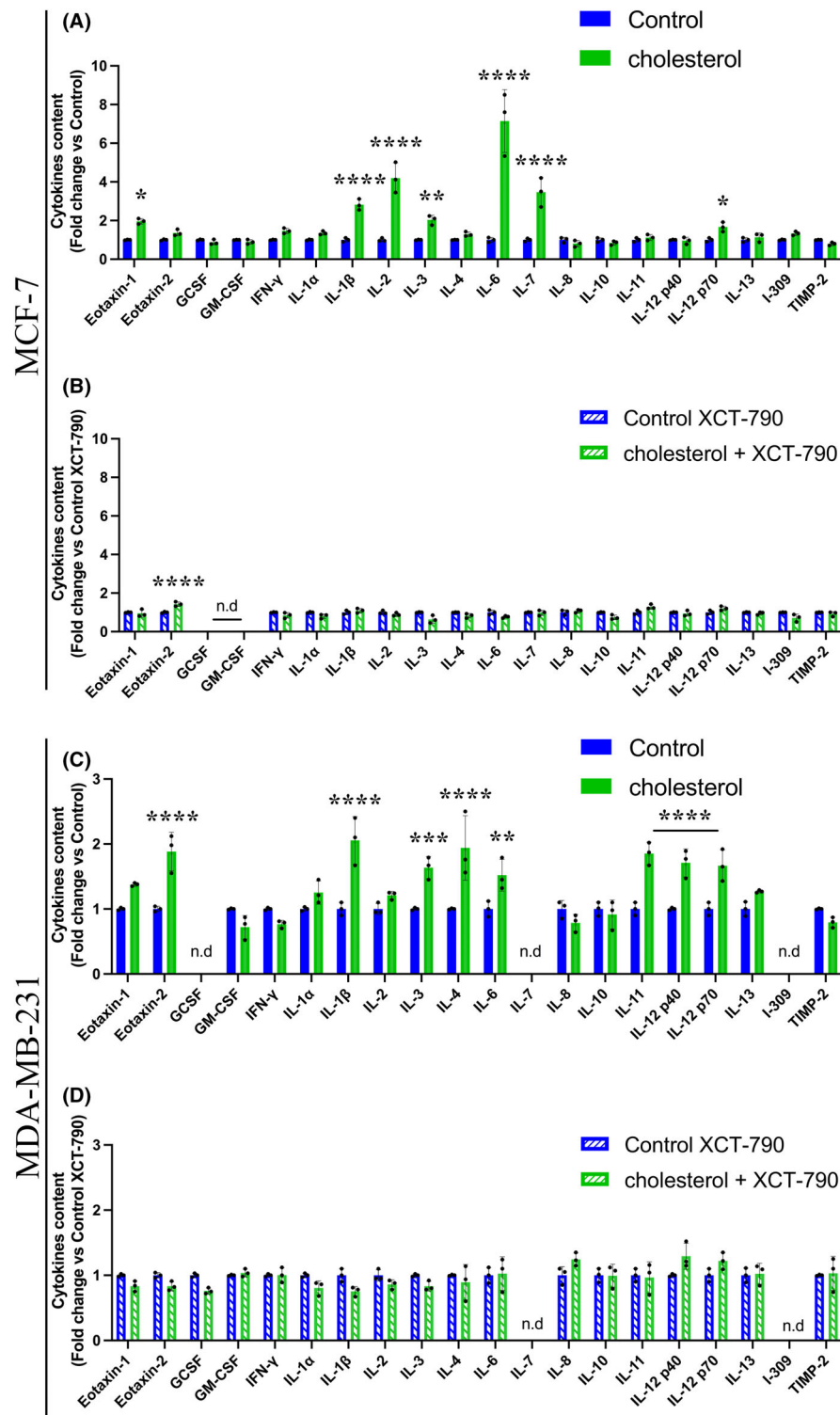


Fig. 2. Cholesterol promotes cytokine release through $ERR\alpha$ activation. Cytokine arrays performed on conditioned media from MCF-7 and MDA-MB-231 treated with EtOH (Control), 10 μ M cholesterol (A, C), 5 μ M XCT-790 (Control XCT-790) or co-treated with 10 μ M cholesterol and 5 μ M XCT-790 (B, D), for 48 h. Values represent the mean \pm SD of three independent experiments ($n = 3$). Statistical analysis was performed using Student's t -test. * P -value < 0.05; ** P -value < 0.01; *** P -value < 0.001; **** P -value < 0.0001; n.d., not detectable.

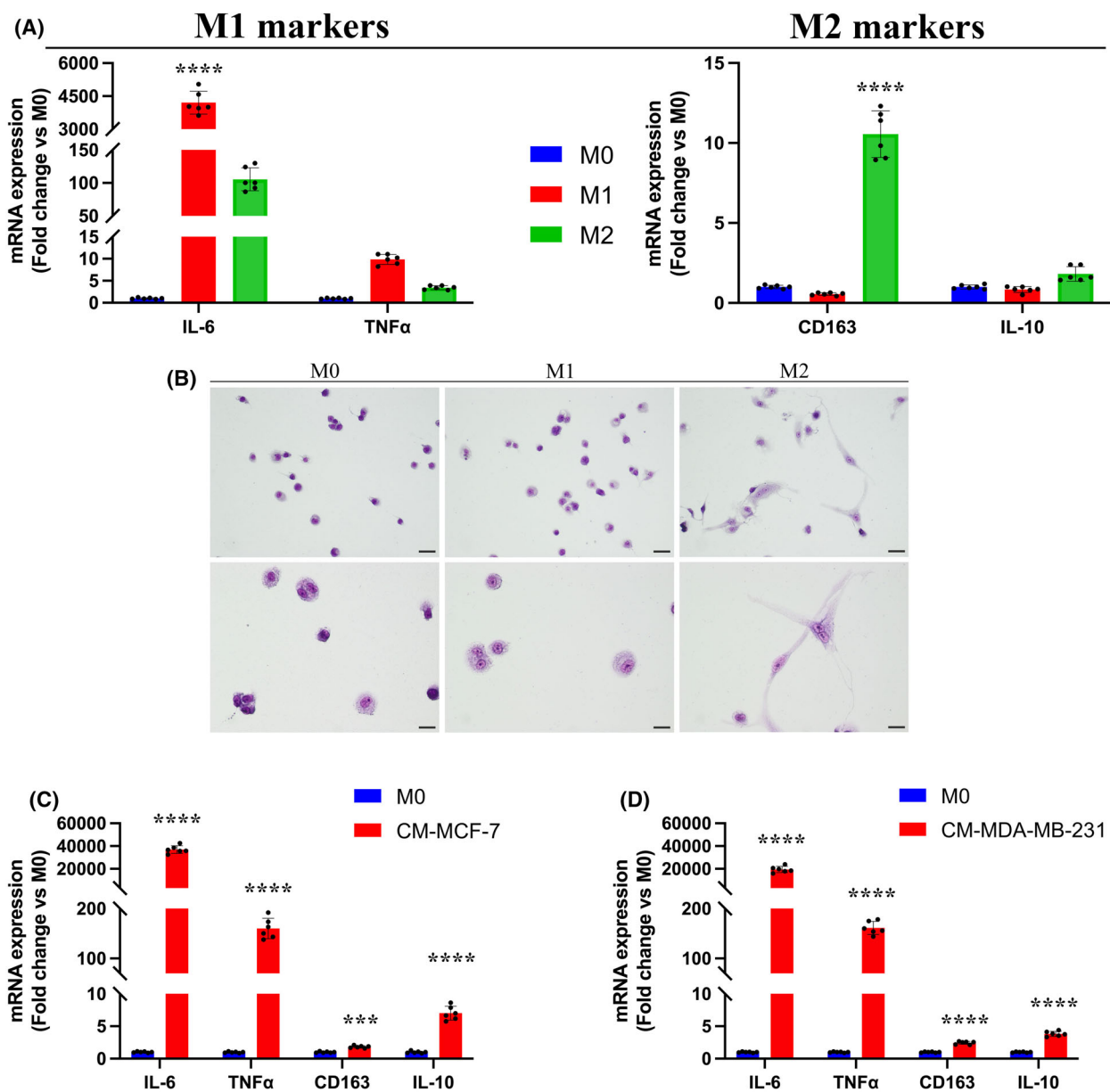
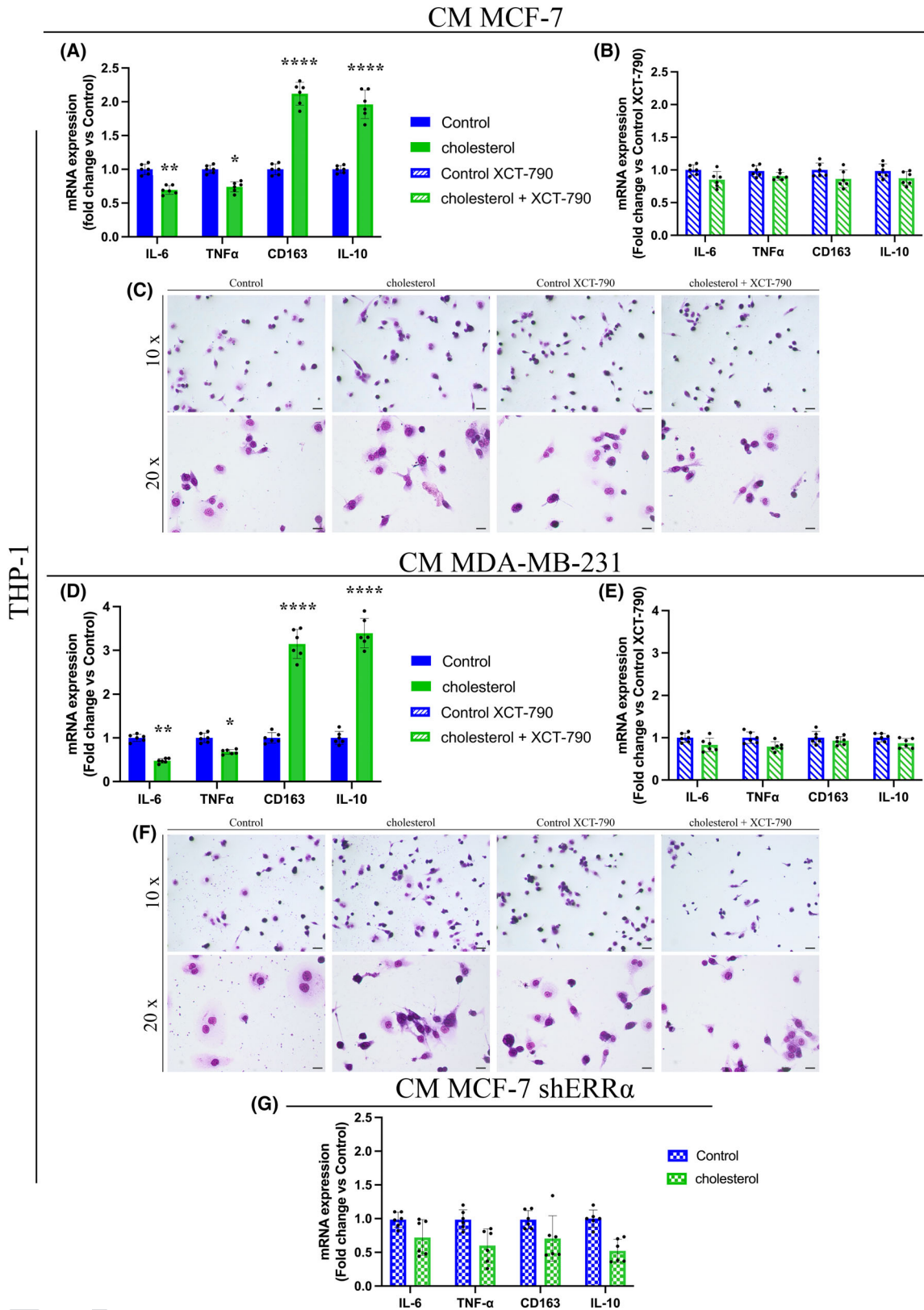


Fig. 3. Breast cancer cell media promote heterogeneous macrophage activation. Real-time analysis (A) and May-Grünwald-Giemsa staining (B) of THP-1 cells treated with 100 nM PMA (M0 stage) and subsequently with 10 ng·mL⁻¹ LPS (M1 stage) or 20 ng·mL⁻¹ IL-4 (M2 stage). Real-time analysis of THP-1 (M0 stage) exposed, for 48 h, to conditioned media from MCF-7 (C) or MDA-MB-231 (D). Values represent the mean \pm SD of three independent experiments ($n = 6$). Statistical analysis was performed using one-way ANOVA analysis (A) or Student's *t*-test (C, D). * *P*-value < 0.05; ** *P*-value < 0.01; *** *P*-value < 0.001; **** *P*-value < 0.0001.

Cholesterol enhances the cancer-associated fibroblast (CAF) phenotype, through ERR α pathway activation

Given the results on macrophages, we next evaluated the effects mediated by the culture media from MCF-7 and MDA-MB-231 cells exposed to cholesterol on the fibroblasts, another cell component of the environment

surrounding the tumour. Fibroblasts play very important physiological roles as they give stability to different tissues, but they also play a pivotal role in neoplastic progression as they provide advantages for tumour cells, guaranteeing physical stability as well as the supply of metabolites useful for its progression [27,28]. The cultured media, from cholesterol-treated



THP-1

color

Fig. 4. Breast cancer cells exposed to cholesterol treatment induce M2 phenotype in THP-1 cells. Real-time analysis (A, B) and May-Grünwald-Giemsa staining (C) of THP-1 (M0 stage) exposed, for 48 h, to conditioned media from MCF-7 previously treated with EtOH (Control), 10 μM cholesterol, or co-treated with 10 μM cholesterol and 5 μM XCT-790, for 48 h. Pictures were taken at 10 \times or 20 \times magnification, and scale bars are 50 or 25 μm , respectively. Real-time analysis (D, E) and May-Grünwald-Giemsa staining (F) of THP-1 (M0 stage) exposed, for 48 h, to conditioned media from MDA-MB-231 previously treated with EtOH (Control), 10 μM cholesterol, or co-treated with 10 μM cholesterol and 5 μM XCT-790, for 48 h. Pictures were taken at 10 \times or 20 \times magnification and scale bars are 50 or 25 μm , respectively. (G) Real-time analysis of THP-1 (M0 stage) exposed for 48 h to conditioned media from MCF-7 shERR α previously treated with EtOH (Control) or 10 μM cholesterol for 48 h. Values represent the mean \pm SD of three independent experiments ($n = 6$). Statistical analysis was performed using Student's t -test. * P -value < 0.05; ** P -value < 0.01; **** P -value < 0.0001.

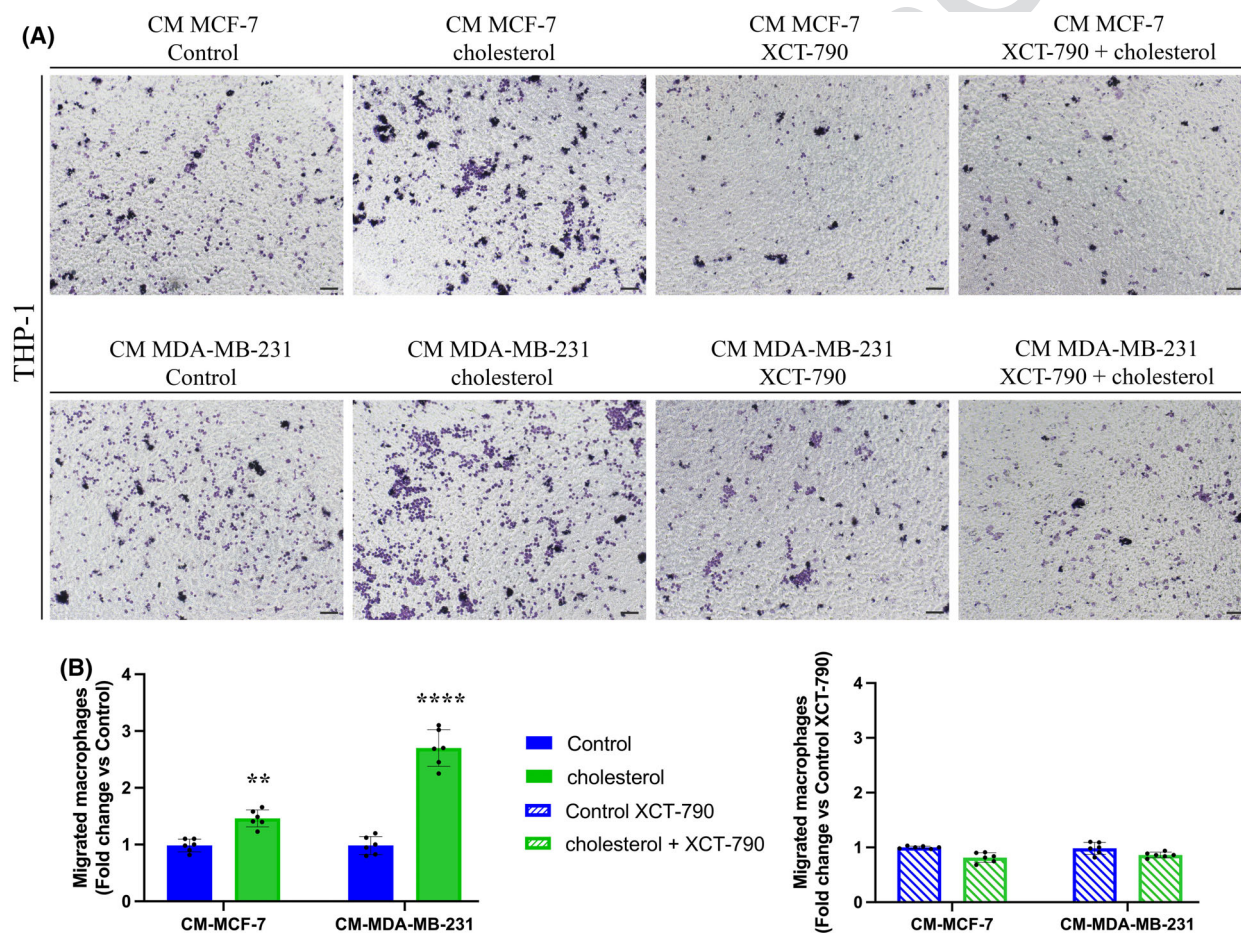


Fig. 5. Breast cancer cells exposed to cholesterol treatment promoted macrophage chemotaxis. (A) Chemotaxis effects on THP-1 cells mediated by conditioned media from MCF-7 and MDA-MB-231 cells previously treated with EtOH (Control), 5 μM XCT-790 (Control XCT-790), 10 μM cholesterol, or co-treated with 10 μM cholesterol and 5 μM XCT-790, for 48 h. Pictures were taken at 10 \times magnification and scale bars are 50 μm . (B) Migrated macrophage quantification. Results obtained were related to their own control. Values represent the mean \pm SD of three independent experiments ($n = 6$). Statistical analysis was performed using Student's t -test. ** P -value < 0.01; **** P -value < 0.0001.

breast cancer cell lines, was used to culture the BJ hTERT human fibroblast cell line.

The mRNA levels of typical fibroblast activation markers in CAFs were then assessed. The results displayed that fibroblasts treated with the media from breast cancer cells exposed to cholesterol showed marked increases in the

mRNA levels of α -smooth muscle actin (α -SMA), fibroblast activation protein (FAP), as well as transforming growth factor- β (TGF- β) and metalloproteinase-9 (MMP-9), ranging from 2-fold to more than 4-fold for FAP in MDA-MB-231, with respect to their own control (Fig. 6 panels A,C). Conversely, these results did not

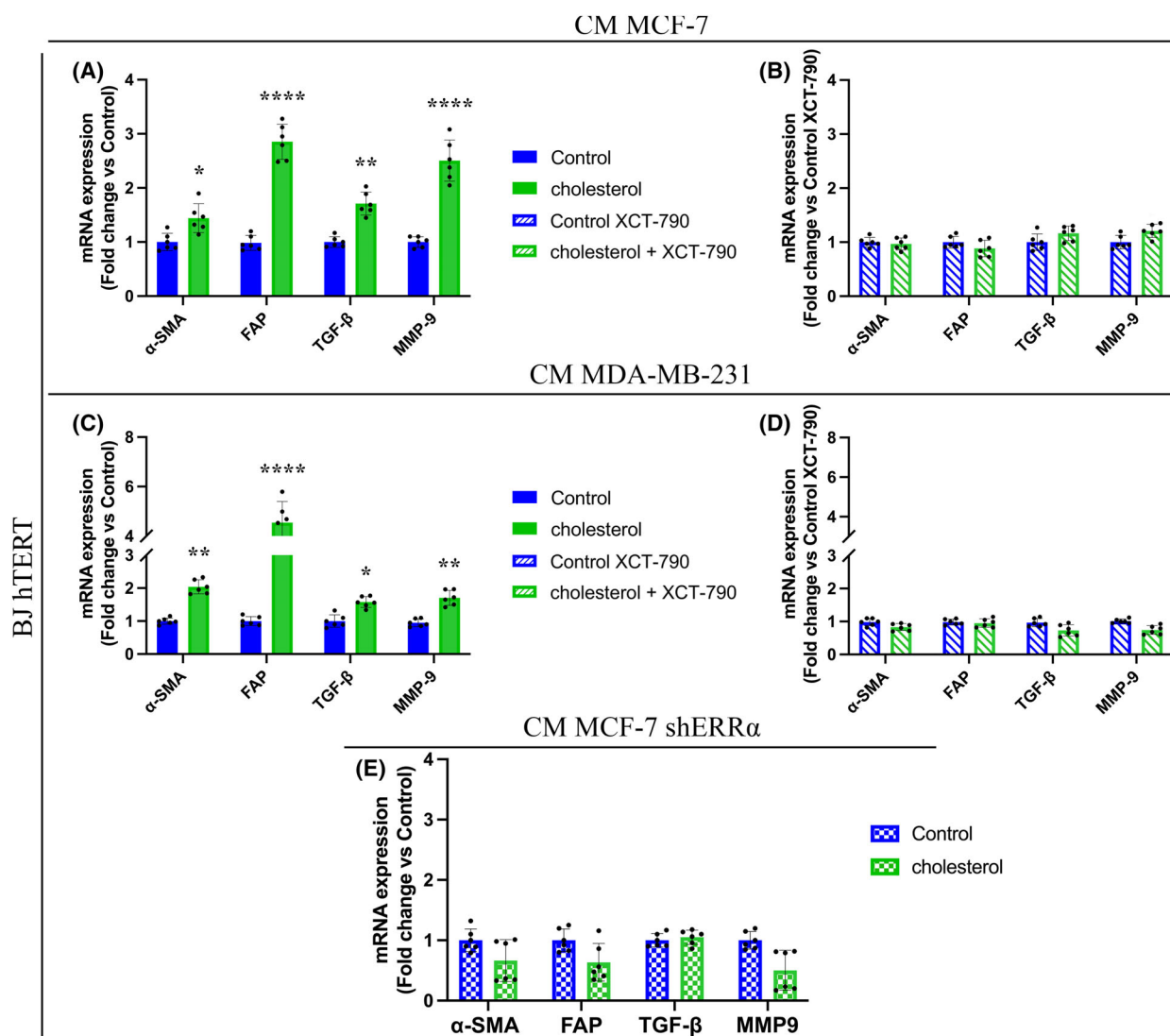


Fig. 6. Breast cancer cells exposed to cholesterol treatment induce CAF phenotypes in BJ hTERT cells. Real-time analysis of BJ hTERT cells treated, for 48 h, with conditioned media from MCF-7 and MDA-MB-231 previously treated with EtOH (Control), 10 μ M cholesterol (A, C), 5 μ M XCT-790 (Control XCT-790) or co-treated with 10 μ M cholesterol and 5 μ M XCT-790 (B, D), for 48 h. (E) Real-time analysis of BJ hTERT cells treated for 48 h with conditioned media from MCF-7 shERR α previously treated with EtOH (Control) or 10 μ M cholesterol. Values represent the mean \pm SD of three independent experiments ($n = 6$). Statistical analysis was performed using Student's t -test. * P -value < 0.05; ** P -value < 0.01; **** P -value < 0.0001.

occur after treatment of BJ hTERT with the media from MCF-7 and MDA-MB-231 cells exposed to XCT-790 alone compared to those exposed to XCT-790 and cholesterol simultaneously, highlighting again that XCT-790 is able to prevent the effects induced by cholesterol (Fig. 6 panels B,D). Outcomes were also confirmed on MCF-7 shERR α . As shown in Fig. 6 panel E, after treatment of BJ hTERT with the media from MCF-7 shERR α cells exposed to cholesterol, mRNA levels of α -SMA, FAP, TGF- β and MMP-9 resulted stable as obtained during XCT-790 co-treatment.

The activation of fibroblasts to CAFs is also characterized by metabolic mitochondrial changes and reactive oxygen species (ROS) production [46,47]. For this purpose, using the MitoTracker Orange fluorescent probe, the mitochondrial potential was evaluated in BJ hTERT cells after treatment with the conditioned media from MCF-7 and MDA-MB-231 cells exposed or not to cholesterol. The results in Fig. 7 show that the conditioned media of both treated breast cancer lines were able to reduce mitochondrial membrane potential (Fig. 7 panels A,B), indicating reduced

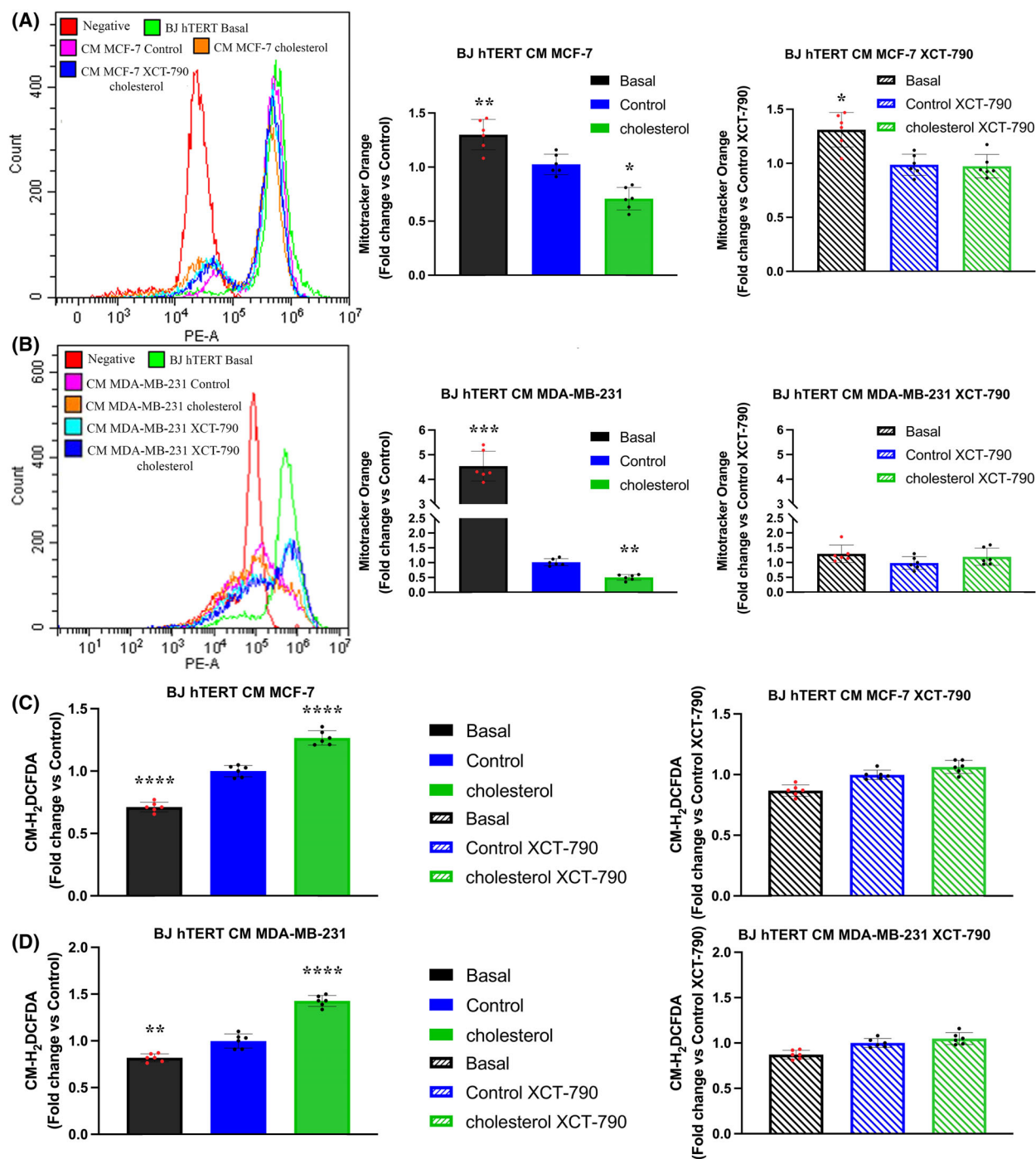


Fig. 7. Cholesterol treatment of breast cancer cells reduces mitochondrial potential and promotes reactive oxygen species production, cancer-associated fibroblast features, in BJ hTERT cells. Mitochondrial potential of BJ hTERT, assessed using MitoTracker Orange CM-H₂TMRos probes, after 48 h of exposition to conditioned media from MCF-7 (A) and MDA-MB-231 (B) previously treated with EtOH (Control), 5 μ M XCT-790 (Control XCT-790), 10 μ M cholesterol, or 10 μ M cholesterol and 5 μ M XCT-790, for 48 h. ROS intracellular levels in BJ hTERT, assessed using CM-H₂DCFDA probes, after 48 h of exposition to conditioned media from MCF-7 (C) and MDA-MB-231 (D) previously treated with EtOH (Control), 5 μ M XCT-790 (Control XCT-790), 10 μ M cholesterol, or 10 μ M cholesterol and 5 μ M XCT-790, for 48 h. Values represent the mean \pm SD of three independent experiments ($n = 6$). Statistical analysis was performed using one-way ANOVA analysis. * P -value < 0.05; ** P -value < 0.01; *** P -value < 0.001; **** P -value < 0.0001.

mitochondrial function, a metabolic characteristic of CAFs [48]. The activation of fibroblasts turned out to be driven by a direct action of cholesterol on $ERR\alpha$ since this reduction in mitochondrial potential was not evident after treatment with the media from MCF-7 and MDA-MB-231 cells exposed to XCT-790 and cholesterol, simultaneously, compared to those exposed to XCT-790 alone. In addition to this, and given the fundamental role of ROS, another hallmark of CAFs, that normally increases in this cell phenotype [46,47], we evaluated whether the conditioned media of breast cancer cells exposed to cholesterol was able to promote ROS production. To this end, the BJ hTERT was treated with the conditioned media from MCF-7 and MDA-MB-231 cells exposed or not to cholesterol, and ROS levels were evaluated by using the CM-H₂-DCFDA fluorescent probe. The results show that the treatment is able to increase ROS levels (Fig. 7 panel C,D) while the treatment of BJ hTERT with the media from MCF-7 and MDA-MB-231 cells exposed to XCT-790 alone compared to those exposed to XCT-790 and cholesterol did not show significant differences (Fig. 7 panel C,D).

Cholesterol drives angiogenesis, through $ERR\alpha$ pathway activation

Tumour endothelial cells (TECs) are significant components of the tumour microenvironment [30]. They are able to coordinate and promote the formation of a new endothelium, a feature exploited by the tumour to promote the supply of more nutrients and oxygen as well as to use the bloodstream in order to disseminate cells throughout the organism, providing a competitive advantage over distant metastasis onset [30,49]. Given the already significant activity shown by the conditioned media from breast cancer exposed to cholesterol to rearrange the two previous cell lines constituting the microenvironment, we evaluated whether TECs were also affected by these treatments in such a way as to orchestrate a pro-tumoral microenvironment. To do this, the Ea Hy926 endothelial cell line was used. The cells were treated with the conditioned media from MCF-7 and MDA-MB-231 cells treated or not with 10 μ M cholesterol for 48 h, and the tube formation assay was used to assess their ability to determine the formation of new vessels.

As shown in Fig. 8 (panel A), the conditioned media from treated breast cancer cells was found to be able to promote tube formation, which did not occur when Ea Hy926 cells were treated with the conditioned media from cells co-treated with cholesterol and XCT-790.

Furthermore, the tube formation is driven by intense glycolytic activity and poor mitochondrial activity [50,51]. In this regard, the mitochondrial potential was evaluated by using the MitoTracker Orange fluorescent probe. In detail, the mitochondrial membrane potential of Ea Hy926 cells was assessed following treatment with the conditioned media from MCF-7 and MDA-MB-231 cells exposed or not to cholesterol. The results in Fig. 8 (panels B,C) showed that the culture media from both breast cancer lines was able to reduce the mitochondrial membrane potential showing reduced mitochondrial function, a metabolic feature of active endothelial cells. However, this reduction in membrane mitochondrial potential was not evident after treatment with media from MCF-7 and MDA-MB-231 cells exposed to XCT-790 alone compared to those simultaneously exposed to XCT-790 and cholesterol (Fig. 8 panels B,C).

In addition to the tube formation evaluation, we also evaluated the ability of endothelial cells to lead to sprouting, that is the ability of the cell to stretch and remodel in order to subsequently promote the formation of new vessels. The results showed a trend comparable to that highlighted in the previous tube formation experiments (Fig. 9). The sprouting process of the endothelial cell represents the primary event which then converges in the formation of a new endothelium [50,51].

Discussion

Relapses, metastases and tumour resistance are limiting factors in current drug treatments against neoplasms [52,53]. Therefore, world scientific research is focused on identifying the mechanisms driving these processes in order to establish new and efficient therapies.

Several current reports underline the key role of metabolic reprogramming in the processes leading to both tumour progression and its metastasizing power [52,53]. This latter, together with greater aggressiveness, as well as depending on the metabolic switches typical of the neoplasm, has also been seen to be due to various features that the tumour acquires during its growth, through a process known as epithelial-mesenchymal transition (EMT) [54,55]. In this scenario, our recent report fits, highlighting how high cholesterol levels, through $ERR\alpha$ activation, were able to drive an intense metabolic rearrangement causing greater breast cancer cell proliferation, metastasizing power and resistance to the main pharmacological treatments [21]. In continuity with our previous report, this study aimed to evaluate, for the first time, the

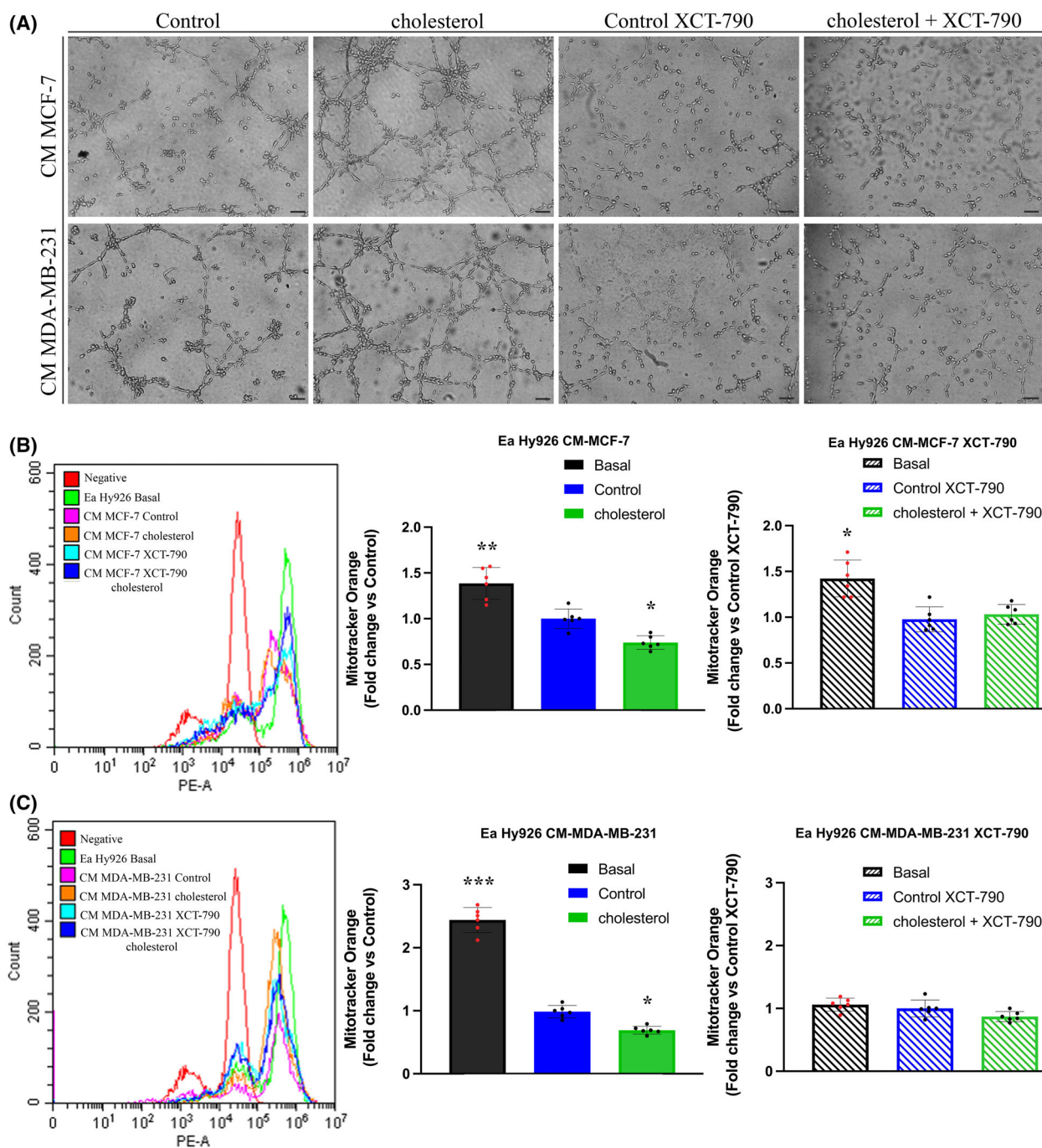


Fig. 8. Breast cancer cells exposed to cholesterol treatment promote the angiogenic process in Ea Hy926. (A) Tube formation in Ea Hy926 cells after 24 h of exposure to conditioned media from MCF-7 or MDA-MB-231 previously treated with EtOH (Control), 5 μM XCT-790 (Control XCT-790), 10 μM cholesterol, or 10 μM cholesterol and 5 μM XCT-790, for 48 h. Pictures were taken at 10x magnification, and scale bars are 50 μm. (B) Mitochondrial potential of Ea Hy926, assessed using MitoTracker Orange CM-H₂TMRos probes, after 48 h of exposition to conditioned media from MCF-7 and MDA-MB-231 (C) previously treated with EtOH (Control), 5 μM XCT-790 (Control XCT-790), 10 μM cholesterol, or 10 μM cholesterol and 5 μM XCT-790, for 48 h. Values represent the mean ± SD of three independent experiments (*n* = 6). Statistical analysis was performed using one-way ANOVA analysis. **P*-value < 0.05; ***P*-value < 0.01; ****P*-value < 0.001.

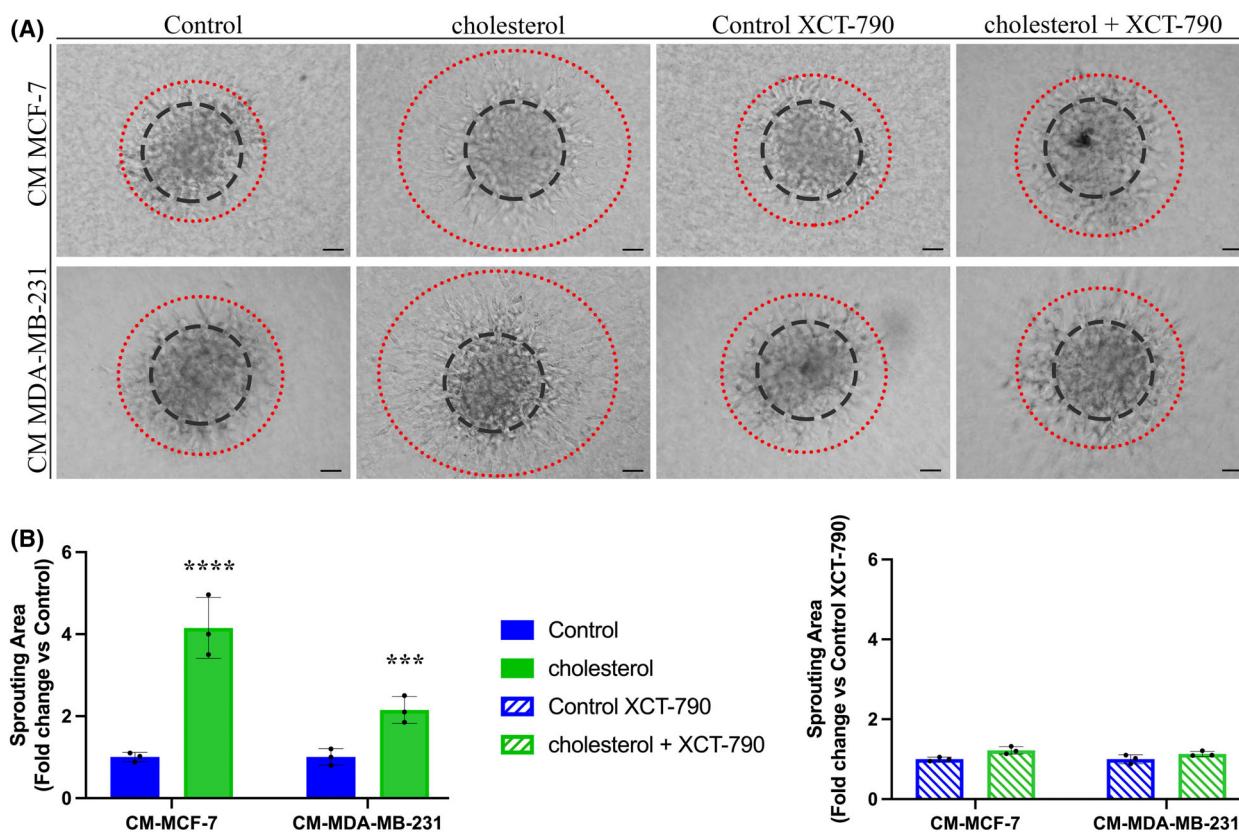


Fig. 9. Breast cancer cells exposed to cholesterol promote endothelial sprouting. (A) Sprouting formation assay in Ea Hy926 cells after 24 h of exposure to conditioned media from MCF-7 or MDA-MB-231 previously treated with EtOH (Control), 5 μ M XCT-790 (Control XCT-790), 10 μ M cholesterol, or 10 μ M cholesterol and 5 μ M XCT-790 for 48 h. Black rings represent spheroids area; red rings represent sprouting area. Pictures were taken at 20 \times magnification, and scale bars are 25 μ m. (B) Sprouting area quantification. Results obtained were related to their own control. Values represent the mean \pm SD of three independent experiments. Statistical analysis was performed using Student's *t*-test. ****P*-value < 0.001; *****P*-value < 0.0001.

effects mediated by cholesterol in promoting EMT. It is now widely known that the EMT process is characterized by various distinct protein markers, notably vimentin, whose overexpression is related to greater tumour aggressiveness [56,57]. Moreover, decreased expression levels of E-cadherin, a membrane glycoprotein, appear to be linked to noticeable cell motility, as well as resistance to apoptotic processes [58,59], these both being features that contribute to greater tumour aggressiveness. Besides these, the Zinc finger E-box-binding homeobox 1 (ZEB-1) protein plays a pivotal role, its expression levels increasing when E-cadherin expression decreases [60,61]; it is also associated with marked cell motility, confirming activation of the EMT process.

Here, we proved that, in MCF-7 and MDA-MB-231 breast cancer cells, by activating the $ERR\alpha$ pathway, cholesterol excess promotes the induction of the above-mentioned markers of the EMT process, both

at transcriptional and translational level, as well as the secretion of MMP-9, that is one of the main metalloproteinases, dedicated to extracellular matrix remodelling [62]. These results support a role for cholesterol in mediating cancer aggressiveness.

However, the tumour should not be evaluated as a separate entity from the surrounding environment as it itself is affected by neighbouring cells and *vice versa* [25,63]. According to Paget's theory and based on several reports published in recent years, the tumour tries to create an almost parasitic relationship between itself and the cells that make up the microenvironment, in order to promote the growth, as well as the possible dissemination of the cancer cells [22,23,64].

In this context, the greater tumour aggressiveness, as well as its metastasizing power, do not derive only from internal characteristics of the tumour itself but also from the surrounding microenvironment, which is constantly stimulated by the tumour cells [22,64]. In

1 this context, our findings demonstrated that breast
2 cancer cells exposed to high cholesterol levels were
3 able to release a huge amount of inflammatory cytokines
4 into the surrounding environment, as well as soluble
5 factors which lead to inflammatory processes in
6 close proximity to the tumour. Additionally, the
7 release of the soluble factors was ascribed to a direct
8 effect of cholesterol on the $ERR\alpha$ pathway, as the
9 simultaneous treatment of tumour cells with cholesterol
10 and XCT-790, a known inverse agonist of $ERR\alpha$,
11 was able to abolish these effects. The massive release
12 of both soluble factors and pro-inflammatory cytokines
13 prompted the hypothesis that high cholesterol
14 levels could induce breast cancer cells to activate cells
15 adjacent to the tumour, thus generating a pro-tumour
16 microenvironment.

17 Therefore, the present work aimed to evaluate, for
18 the first time, whether high cholesterol levels could
19 promote the main components that make up the
20 microenvironment. For this purpose, different stromal
21 cell types, such as macrophages, fibroblasts and
22 endothelial cells, were exposed to conditioned media
23 from breast cancer cells previously treated with
24 cholesterol and their features were assessed. It is
25 known that the continuous secretion of pro-inflammatory
26 cytokines by the tumour and the hypoxic conditions
27 found in the immediate proximity of the neoplastic
28 tissue promotes the polarization of macrophages in
29 tumour-promoting M2 macrophages (M2 phenotype)
30 which in turn will support neoplastic progression [65].
31 Our results displayed intense M2-type macrophage
32 activation, as evidenced by the identification, at
33 transcriptional level, of typical markers of this
34 phenotype, as well as by the findings of morphological
35 changes. Furthermore, a notable chemotactic effect
36 produced by the conditioned tumour media against
37 monocyte cells was highlighted, underlining a greater
38 macrophage component in the tumour site, a feature
39 that very often causes negative prognosis [66].
40 Furthermore, in our experimental model, it was
41 observed that fibroblasts, after treatment with
42 conditioned media from the breast cancer cells
43 exposed to cholesterol, significantly increased mRNA
44 levels of markers characterizing the activation of
45 fibroblasts in CAFs, such as α -smooth muscle actin
46 (α -SMA), fibroblast activation protein (FAP),
47 as well as transforming growth factor- β (TGF- β)
48 and metalloproteinase-9 (MMP-9). In addition,
49 the same treatment evidenced both a lowering of
50 the mitochondrial membrane potential typical of
51 tumour-associated fibroblasts, as their metabolism
52 is mainly glycolytic, and an increase in the
53 production of reactive oxygen species, two

features peculiar to CAFs [67,68]. Lastly, in accordance
with literature evidence highlighting that tumour
angiogenesis plays a critical role during cancer
progression [69,70], our outcomes displayed a clear
tendency of endothelial cells to organize themselves
to form new vessels, as evidenced by the tube
formation assay. They also showed a greater ability
to determine endothelial branching, confirmed by
both the sprouting experiments and the intense
reduction in the mitochondrial potential, indicative
of a greater predilection for the glycolytic metabolism
peculiar to these processes.

Notably, the present work demonstrates that the
intense effects induced by cholesterol in driving the
EMT process and microenvironment orchestration are
due to a direct effect of cholesterol on the $ERR\alpha$
pathway of breast cancer cells. This is supported by
the outcomes obtained following co-treatment with
XCT-790, as well as by the results of the experiments
performed on MCF-7 sh $ERR\alpha$, in which the direct
effect of cholesterol on $ERR\alpha$ was proved without
any external perturbation.

Taken together, these results underline that high
cholesterol levels, through $ERR\alpha$ activation, can
determine greater tumour aggressiveness by directly
promoting the EMT process of tumour cells, as well
as by inducing an intense microenvironment
orchestration.

The results of this report fit into an even broader
context, attempting to give further elucidations
about the role of the mevalonate pathway in driving
malignant transformation [71–73]. There are several
reports according to which the inhibition of this
pathway could lead to interesting anti-tumour
effects. Statins are well-established drugs commonly
used to reduce serum cholesterol level by
inhibiting the HMGCR enzyme [74], and they also
appeared to be able to exert antitumour effects in
human malignancies, including breast cancer [75,76].
However, the role of statins is debatable; indeed,
other studies have failed to show any significant
anti-tumour effects [77]. Preclinical and clinical
studies on breast malignancies demonstrated
variable effects of statins, depending on the cell
lines and cohorts [78,79].

The results of this report, on the one hand, highlight
how high cholesterol levels promote greater tumour
aggressiveness, thus confirming the relevance of the
mevalonate pathway in tumour progression; on the
other hand, they suggest $ERR\alpha$ as a possible new
molecular target for the treatment of breast
carcinoma, thus paving the way for a new
therapeutic approach that is not based directly on
the reduction of cholesterol levels, but aims at
targeting the main pro-tumoural targets.

Materials and Methods

Cell cultures

All cell lines used in this work (MCF-7, MDA-MB-231, THP-1, BJ hTERT and Ea Hy926) were purchased from the American Culture Collection (ATCC, Manassas, VA, USA) and were cultured at 37 °C in 5% CO₂ in a humidified atmosphere. For the maintaining purpose, cells were cultured as follows: MCF-7 and MDA-MB-231 cells were cultured in DMEM/F12 (Sigma Aldrich, St. Louis, MO, USA) supplemented with 10% foetal bovine serum (FBS, Sigma Aldrich), 2 mM L-glutamine (Gibco, Life Technologies, Waltham, MA, USA), and 1% penicillin/streptomycin (Gibco, Life Technologies). BJ hTERT and Ea Hy926 cells were cultured in DMEM-high glucose (Sigma Aldrich) supplemented with 10% FBS, 2 mM L-glutamine and 1% penicillin/streptomycin. THP-1 cells were cultured in RPMI-1630 (Sigma Aldrich) supplemented with 10% Fetal Bovine Serum, 4 g·L⁻¹ glucose (Sigma Aldrich), 10 mM HEPES (Sigma Aldrich), 1 mM sodium pyruvate (Sigma Aldrich), 0.05 mM mercaptoethanol (Sigma Aldrich). Two millimolar L-glutamine and 1% penicillin/streptomycin.

Real-time analysis

MCF-7 and MDA-MB-231 cells were grown in 10 cm dishes to 70–80% confluence and exposed for 48 h to the vehicle (EtOH), 10 μM cholesterol, 5 μM XCT-790 or co-treated with 10 μM cholesterol and 5 μM XCT-790. Total cellular RNA was extracted using TRIZOL reagent (Sigma-Aldrich), according to the manufacturer's instructions. RNA purity and integrity were assayed both spectroscopically and by gel electrophoresis. Complementary DNA (cDNA) was synthesized by reverse transcription of 2 μg of RNA template, if its OD 260/280 ranged from 1.8 to 2.0. Gene expression analysis was performed using the Quant Studio7 Flex Real-Time PCR System platform (Life Technologies) using SYBR Green Universal PCR Master Mix (Roche, Monza, MB, Italy), as previously described [80]. Relative mRNA levels were calculated using the $\Delta\Delta C_t$ method and comparing it with the control group. The $2^{-\Delta\Delta C_t}$ was used to calculate the relative expression of each gene, and the ΔC_t values were determined by subtracting the average C_t values of the endogenous control gene *18s* from the average C_t values of each gene type. All the primers used for amplifications are listed in Table 1. Real-Time analysis was also performed in THP-1 treated with 100n PMA, 10 ng·mL⁻¹ LPS, 20 ng·mL⁻¹ IL-4 or with the conditioned media from MCF-7 and MDA-MB-231 cells previously treated as described above. Gene expression analysis was also performed in BJ hTERT treated with the conditioned media from MCF-7 and MDA-MB-231 cells previously treated as described above.

Table 1. qPCR Primers.

Primer name	Sequence (5'-3')
Vimentin Fw	AGAACCTGCAGGAGGCAGAAGAAT
Vimentin Rv	TTCCATTTACGCATCTGGCGTTC
E-cadherin Fw	CCCACCACGTACAAGGGTC
E-cadherin Rv	ATGCCATCGTTGTTCACTGGA
ZEB-1 Fw	GCACAACCAAGTGAGAAGA
ZEB-1 Rv	GCCTGGTTCAGGAGAAGATG
MMP-9 Fw	ATTTCTGCCAGGACCGCTTCTACT
MMP-9 Rv	CAGTTTGTATCCGGCAAAGTGGCT
IL-6 Fw	AACCTGAACCTTCCAAAGATGG
IL-6 Rv	TCTGGCTTGTTCCTCACTACT
TNF-α Fw	ATGAGCACTGAAAGCATGATCC
TNF-α Rv	GAGGGCTGATTAGAGAGAGGTC
CD-163 Fw	ACTTGAAGACTCTGGATCTGCT
CD-163 Rv	CTGGTGACAAAACAGGCACTG
IL-10 Fw	ACTTTAAGGGTTACCTGGGTTGC
IL-10 Rv	TCACATGCGCCTTGATGTCTG
α-SMA Fw	GCAGCCCAGCCAAGCACTGT
α-SMA Rv	TGGGAGCATCGTCCCAGCA
FAP Fw	AGAAAGCAGAAGCTGGAGG
FAP Rv	ACACACTTCTTGCTTGGAGGAT
TGF-β Fw	GGTTTTCCGCTTCAATGTGT
TGF-β Rv	GCTCGATCCTCTGCTCATT
18S Fw	AGTCGGAGGTTCAAGACGAT
18S Rv	GCGGGTCATGGGAATAACG

shRNA lentiviral transduction

Packaging cells (293Ta), reagents and lentiviral plasmids were purchased from GeneCopoeia (Product ID. HSH095573) 293Ta cells were seeded and left in culture for 48 h. Then, packaging cells were transfected with lentiviral vectors encoding an shRNA clone set of two constructs against human ESRRRA gene, coding for ERRα, in a lentiviral psi-LVRInU6TGP vector, with an inducible U6 promoter, CMV promoter-TetR-SV40 promoter-eGFP-IRES-puromycin. A scrambled control psi-LVRInU6TGP vector (Scramble) was transfected in parallel. Two days post-transfection, the lentivirus-containing culture medium was filtered through a 0.45 μm filter and added to the target cells (MCF-7), in the presence of 5 μg·mL⁻¹ Polybrene. Infected cells were selected, with 1.5 μg·mL⁻¹ puromycin. Positive clones were then subjected to immunoblot analysis in order to confirm the proper silencing of ERRα.

Immunoblot analysis

For the immunoblot analysis performed in this study, cells were grown to 70–80% confluence and treated with EtOH (Control), 10 μM cholesterol, 5 μM XCT-790 (Control XCT-790) or co-treated with 10 μM cholesterol and 5 μM XCT-790 for 48 h. Then, cells were harvested and lysed in 100 μL of lysis buffer to produce the total cell lysates (50 mM Tris-HCl, 150 mM NaCl, 1% NP-40, 0.5% sodium deoxycholate,

2 mm sodium fluoride, 2 mm EDTA, 0.1% SDS), as previously described [81]. The same amounts of proteins, quantified by the Bradford assay, as previously described [82], from total lysates, were resolved on SDS-polyacrylamide gel, as previously described [83], transferred to a nitrocellulose membrane and probed with anti-Vimentin (sc-6260), anti-E-cadherin (sc-8426), anti ZEB1 (sc-515797), anti-ERR α (ab76228; Santa Cruz, Biotechnology; Abcam, Cambridge, UK). The equal loading and transfer was verified by incubation with the anti- β -actin antibody (Santa Cruz, Biotechnology). The antigen and antibody complex was detected by incubation of the membranes with IR peroxidase-coupled goat anti-mouse or goat anti-rabbit antibodies and was revealed using the Li-COR system (Li-COR Biosciences, Lincoln, NE, USA). Subsequently, the bands of interest were quantified using IMAGEJ software.

Gel-Zymography

MCF-7 and MDA-MB-231 cells were grown in 24-well plates to 70–80% confluence and then washed twice with PBS and treated (in FBS-free media) for 48 h with vehicle (EtOH), 10 μ M cholesterol, 5 μ M XCT-790 or co-treated with 10 μ M cholesterol and 5 μ M XCT-790. At the end of treatment, the conditioned media was collected and centrifuged to eliminate dead cells. Samples were added with 5 \times non-reducing sample buffer (4% SDS, 20% glycerol, 0.01% bromophenol blue and 125 mM Tris-HCL, pH 6.8), loaded into gelatin-acrylamide gel and exposed to a 150 V electrophoresis run. Then, the gel was washed twice, for 30 min each, in washing buffer (2.5% Triton X-100, 50 mM Tris-HCL, pH 7.5, 5 mM CaCl₂, 1 μ M ZnCl₂). At the end of the washing procedures, the gel was rinsed with incubation buffer (1% Triton X-100, 50 mM Tris-HCL, pH 7.5, 5 mM CaCl₂, 1 μ M ZnCl₂) and left at 37 °C, for 24 h. After 24 h of incubation, gel was stained in Coomassie blue solution and then destained until bands could be clearly seen. The gel was then scanned, and band densities were quantified using software. Data were normalized to cell mass determined by using the Sulforhodamine B (SRB) assay.

Cytokine arrays

Cytokine production was assessed in the culture media using the RayBio[®] Human inflammation array kit, following the manufacturer's instructions. Briefly, MCF-7 and MDA-MB-231 cells were grown in 6-well plates to 80% confluence and then treated for 48 h with vehicle (EtOH), 10 μ M cholesterol, 5 μ M XCT-790 or co-treated with 10 μ M cholesterol and 5 μ M XCT-790. At the end of treatment, the conditioned media was collected and centrifuged to eliminate dead cells. Simultaneously, the antibody array membranes were incubated in blocking solution for 30 min at room temperature. The blocking solution was then

replaced with the breast-cancer conditioned media and incubated for 3 h at room temperature, under gentle rocking. Membranes were washed twice with wash buffer I and then twice with wash buffer II, for 5 min each. At the end of the washing procedures, the membranes were incubated with biotinylated antibody cocktail at room temperature for 2 h. The membranes were then subjected to the washing procedures described above and incubated with HRP-streptavidin for 2 h. The membranes were then washed, incubated with detection buffer for 2 min and then exposed to a chemiluminescence imaging system. Spot densities were quantified using IMAGEJ software. Data were normalized to cell mass, determined by using the Sulforhodamine B (SRB) assay.

Macrophage differentiation and polarization

In order to obtain differentiated macrophages, THP-1 cells were seeded in 6-well plates in complete media and treated with 100 nM PMA for 24 h. At the end of treatment, the media was replaced and then left for 1 day of rest to reach the M0 stage. The day after, M0 macrophages were stimulated for 6 h with 10 ng·mL⁻¹ LPS or with 20 ng·mL⁻¹ IL-4 for 72 h to generate M1 or M2 macrophages, respectively. Characteristic morphologic changes of monocyte-to-macrophage differentiation were observed and photographed at 10 \times or 20 \times , after May-Grünwald-Giemsa staining, by using phase-contrast microscopy.

Chemotaxis assay

Chemotaxis assays were carried out, using Boyden chambers, on THP-1 cells exposed to conditioned media from MCF-7 and MDA-MB-231 cells. Briefly, 2 \times 10⁵ of MCF-7 or MDA-MB-231 cells were grown in 24-well plates to 80% confluence and then treated for 48 h with vehicle (EtOH), 10 μ M cholesterol, 5 μ M XCT-790 or co-treated with 10 μ M cholesterol and 5 μ M XCT-790. At the end of treatment, the conditioned media was collected and centrifuged to eliminate dead cells. Then, THP-1 cells were seeded in the top portion of the chamber (BD, Bioscience). The lower portion of the chamber contained the previously-prepared conditioned media, used as a chemoattractant. Chambers were incubated at 37 °C for 6 h, washed three times with PBS and stained with May-Grünwald-Giemsa solution. Photographs were taken at 10 \times magnification using phase-contrast microscopy and are representative of three independent experiments.

Mitochondrial membrane potential analysis

To measure the mitochondrial membrane potential, cells were stained with the CM-H₂TMRos (Thermo Fisher) probe, as previously described [21]. The accumulation of

1 the CM-H₂TMRos probe in mitochondria is dependent
2 upon the membrane potential. Briefly, BJ-hTERT and Ea
3 Hy926 exposed were seeded in 6-well plates at 1×10^5
4 cells/well density and treated, for 48 h, with conditioned
5 media from MCF-7 and MDA-MB-231 cells previously
6 treated with 10 μ M cholesterol, EtOH, 5 μ M XCT-790 or
7 co-treated with 10 μ M cholesterol and 5 μ M XCT-790, for
8 48 h. After treatment, cells were harvested, rinsed and incu-
9 bated in 10 nM MitoTracker Orange solution in PBS for
10 30 min at 37 °C. Samples were then subjected to cytofluorim-
11 etric analysis using the SONY SH800 Cell Sorter (Sony
12 Corporation, Minato, Tokyo, Japan).

14 Reactive oxygen species (ROS) assessment

15 Intracellular ROS were quantified using CM-H₂DCFDA
16 (Thermo Fisher Scientific, Waltham, MA, USA), as pre-
17 viously described [84]. Briefly, 2×10^5 BJ-hTERT cells/
18 well were seeded in 6-well plates and treated for 48 h
19 with the conditioned media coming from MCF-7 or
20 MDA-MB-231 previously treated with vehicle (EtOH),
21 10 μ M cholesterol, 5 μ M XCT-790 or co-treated with
22 10 μ M cholesterol and 5 μ M XCT-790. At the end of
23 treatment, cells were washed with PBS, collected and
24 then resuspended in 5 μ M CM-H₂DCFDA (Thermo
25 Fisher Scientific), a fluorescent dye useful as an indicator
26 for reactive oxygen species, and incubated for 45 min at
27 37 °C. Stained cells were collected by centrifugation, and
28 resuspended in fresh media. Sample fluorescence was
29 quantified with a fluorimeter (Synergy H1 microplate
30 reader, BioTek, Winooski, VT, USA), and fluorescence
31 intensity normalized by viable cell number.

34 Tube formation assay

35 Angiogenesis power was assessed by tube formation assay,
36 as previously described, using conditioned media from
37 MCF-7 or MDA-MB-231 [81]. Briefly, 2×10^5 of MCF-7
38 or MDA-MB-231 cells were grown in 24-well plates to
39 80% confluence and then treated for 48 h with vehicle
40 (EtOH), 10 μ M cholesterol, 5 μ M XCT-790 or co-treated
41 with 10 μ M cholesterol and 5 μ M XCT-790. Simultaneously,
42 Geltrex (Thermo Fisher Scientific) was thawed at 4 °C
43 overnight and used to coat a 96-well plate, which was then
44 incubated at 37 °C for 30 min to solidify. At the end of
45 treatment, conditioned media from MCF-7 and MDA-MB-
46 231 was collected and centrifuged to eliminate dead cells.
47 Then, Ea HY926 cells were trypsinized, washed with PBS
48 to remove trypsin and resuspended in conditioned medium
49 previously obtained from MCF-7 and MDA-MB-231 cells.
50 Thereafter, Ea HY926 cells were plated on the Geltrex
51 (4×10^4 cells/well) and left for 6–8 h, at 37 °C. were pho-
52 tographed. Photographs of the newly formed vascular
53 tube networks were taken at 10 \times magnification using

phase-contrast microscopy and are representative of three
independent experiments.

Spheroid-based sprouting assay

Angiogenesis power was assessed by sprouting assay in Ea
Hy926 exposed to conditioned media from MCF-7 or MDA-
MB-231. Briefly, 2×10^5 of MCF-7 or MDA-MB-231 cells
were grown in 24-well plates to 80% confluence and then
treated for 48 h with vehicle (EtOH), 10 μ M cholesterol, 5 μ M
XCT-790 or co-treated with 10 μ M cholesterol and 5 μ M
XCT-790. The day before the sprouting assay, Ea Hy926
cells were trypsinized and then counted. 8×10^4 Ea Hy926
cells were transferred to 15 mL tubes and resuspended in
fresh media. Then, methylcellulose solution was added and
using a 12-channel pipette, 25 μ L drops of this solution were
seeded onto a 10 cm square Petri dish and then incubated
upside-down at 37 °C for 24 h. The day after, spheroids were
collected, centrifuged and then resuspended in methylcellu-
lose solution supplemented with 20% FBS. The collagen
solution was added to the spheroids and then plated in a
24-well plate. Thereafter, 200 μ L of the previously obtained
conditioned media were placed on the collagen matrix drop-
wise and left for 24 h to stimulate sprouting. The sprouting
assay was stopped by adding 10% paraformaldehyde for
15 min. Then, photographs at 20 \times magnification using
phase-contrast microscopy were acquired and are representa-
tive of three independent experiments.

Statistical analysis

Data are presented as mean values \pm standard deviation,
obtained from ≥ 3 independent experiments, with ≥ 3 repli-
cates per experiment, unless otherwise stated. Statistical anal-
ysis was performed by using Student's *t*-test or analysis of
variance (one-way ANOVA). Normality of each distribution
was confirmed by Shapiro–Wilk's test, while equality of vari-
ance was verified by Welch's or Brown-Forsythe test. Differ-
ences between groups were evaluated by using Bonferroni's
post hoc test. A *P*-value ≤ 0.05 was considered statistically
significant. Data were evaluated using GRAPHPAD PRISM 9.2
(GraphPad Software, Inc., San Diego, CA, USA).

Acknowledgements

Graphical abstract was created with [BioRender.com](https://www.biorender.com).
LF is funded by PAC CALABRIA 2014-2020-Asse
Prioritario 12, Azione B 10.5.12 CUP: H28D19
000040006. We thank Dr Rosita Curcio for her sup-
port in the statistical analysis. **5**

Conflict of interest

The authors declare no conflict of interest.

7 Author contributions

MB, FS, MPL, and ARC were involved in conceptualization; MB, MF, LF, and ARC were involved in data curation; MB, MF, and LF were involved in investigation; LF was involved in revision; FS, MPL, and ARC were involved in supervision; MB and ARC were involved in writing—original draft; VD, FS, and MPL were involved in writing—review and editing. All authors have read and agreed to the published version of the manuscript.

8 Data availability statement

8 XXXX.

References

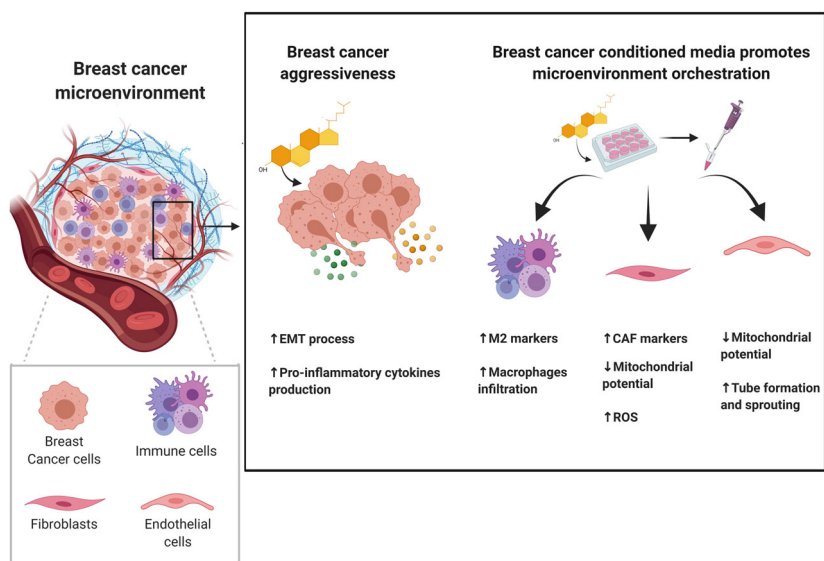
- 1 Cheng C, Geng F, Cheng X, Guo D. Lipid metabolism reprogramming and its potential targets in cancer. *Cancer Commun (Lond)*. 2018;**38**:27.
- 2 Feng Y, Spezia M, Huang S, Yuan C, Zeng Z, Zhang L, et al. Breast cancer development and progression: risk factors, cancer stem cells, signaling pathways, genomics, and molecular pathogenesis. *Genes Dis*. 2018;**5**:77–106.
- 3 Lopez-Garcia MA, Geyer FC, Lacroix-Triki M, Marchio C, Reis-Filho JS. Breast cancer precursors revisited: molecular features and progression pathways. *Histopathology*. 2010;**57**:171–92.
- 4 Dhiman VK, Bolt MJ, White KP. Nuclear receptors in cancer – uncovering new and evolving roles through genomic analysis. *Nat Rev Genet*. 2018;**19**:160–74.
- 5 Robinson-Rechavi M, Escriva Garcia H, Laudet V. The nuclear receptor superfamily. *J Cell Sci*. 2003;**116**:585–6.
- 6 Baek SH, Kim KI. Emerging roles of orphan nuclear receptors in cancer. *Annu Rev Physiol*. 2014;**76**:177–95.
- 7 Wei W, Schwaid AG, Wang X, Wang X, Chen S, Chu Q, et al. Ligand activation of ERRalpha by cholesterol mediates statin and bisphosphonate effects. *Cell Metab*. 2016;**23**:479–91.
- 8 Ranhotra HS. Estrogen-related receptor alpha and cancer: axis of evil. *J Recept Signal Transduct Res*. 2015;**35**:505–8.
- 9 Ranhotra HS. The estrogen-related receptor alpha: the oldest, yet an energetic orphan with robust biological functions. *J Recept Signal Transduct Res*. 2010;**30**:193–205.
- 10 Casaburi I, Chimento A, De Luca A, Nocito M, Sculco S, Avena P, et al. Cholesterol as an endogenous ERRalpha agonist: a new perspective to cancer treatment. *Front Endocrinol (Lausanne)*. 2018;**9**:525.
- 11 Ghanbari F, Mader S, Philip A. Cholesterol as an endogenous ligand of ERRalpha promotes ERRalpha-mediated cellular proliferation and metabolic target gene expression in breast cancer cells. *Cell*. 2020;**9**:1765.
- 12 Liu Y, Ma H, Yao J. ERalpha, a key target for cancer therapy: a review. *Onco Targets Ther*. 2020;**13**:2183–91.
- 13 Tripathi M, Yen PM, Singh BK. Estrogen-related receptor alpha: an under-appreciated potential target for the treatment of metabolic diseases. *Int J Mol Sci*. 2020;**21**:1645.
- 14 Wan Y. PPARgamma in bone homeostasis. *Trends Endocrinol Metab*. 2010;**21**:722–8.
- 15 Bonnelye E, Aubin JE. An energetic orphan in an endocrine tissue: a revised perspective of the function of estrogen receptor-related receptor alpha in bone and cartilage. *J Bone Miner Res*. 2013;**28**:225–33.
- 16 Chang CY, McDonnell DP. Molecular pathways: the metabolic regulator estrogen-related receptor alpha as a therapeutic target in cancer. *Clin Cancer Res*. 2012;**18**:6089–95.
- 17 Ochnik AM, Yee D. Estrogen-related receptor alpha: an orphan finds a family. *Breast Cancer Res*. 2012;**14**:309.
- 18 Tran A, Scholtes C, Songane M, Champagne C, Galarneau L, Levasseur MP, et al. Estrogen-related receptor alpha (ERRalpha) is a key regulator of intestinal homeostasis and protects against colitis. *Sci Rep*. 2021;**11**:15073.
- 19 Suzuki T, Miki Y, Moriya T, Shimada N, Ishida T, Hirakawa H, et al. Estrogen-related receptor alpha in human breast carcinoma as a potent prognostic factor. *Cancer Res*. 2004;**64**:4670–6.
- 20 Misawa A, Inoue S. Estrogen-related receptors in breast cancer and prostate cancer. *Front Endocrinol (Lausanne)*. 2015;**6**:83.
- 21 Brindisi M, Fiorillo M, Frattaruolo L, Sotgia F, Lisanti MP, Cappello AR. Cholesterol and mevalonate: two metabolites involved in breast cancer progression and drug resistance through the ERRalpha pathway. *Cell*. 2020;**9**:1819.
- 22 Friedl P, Alexander S. Cancer invasion and the microenvironment: plasticity and reciprocity. *Cell*. 2011;**147**:992–1009.
- 23 Sounni NE, Noel A. Targeting the tumor microenvironment for cancer therapy. *Clin Chem*. 2013;**59**:85–93.
- 24 Akhtar M, Haider A, Rashid S, Al-Nabet A. Paget's "Seed and Soil" theory of cancer metastasis: an idea whose time has come. *Adv Anat Pathol*. 2019;**26**:69–74.
- 25 Ribelles N, Santonja A, Pajares B, Llacer C, Alba E. The seed and soil hypothesis revisited: current state of knowledge of inherited genes on prognosis in breast cancer. *Cancer Treat Rev*. 2014;**40**:293–9.
- 26 Polyak K, Haviv I, Campbell IG. Co-evolution of tumor cells and their microenvironment. *Trends Genet*. 2009;**25**:30–8.
- 27 Khamis ZI, Sahab ZJ, Sang QX. Active roles of tumor stroma in breast cancer metastasis. *Int J Breast Cancer*. 2012;**2012**:574025.

- 28 Ronca R, Van Ginderachter JA, Turtoi A. Paracrine interactions of cancer-associated fibroblasts, macrophages and endothelial cells: tumor allies and foes. *Curr Opin Oncol*. 2018;**30**:45–53.
- 29 Mantovani A, Schioppa T, Porta C, Allavena P, Sica A. Role of tumor-associated macrophages in tumor progression and invasion. *Cancer Metastasis Rev*. 2006;**25**:315–22.
- 30 Schaaf MB, Houbaert D, Mece O, Agostinis P. Autophagy in endothelial cells and tumor angiogenesis. *Cell Death Differ*. 2019;**26**:665–79.
- 31 Biffi G, Tuveson DA. Diversity and biology of cancer-associated fibroblasts. *Physiol Rev*. 2021;**101**:147–76.
- 32 Kharraishvili G, Simkova D, Bouchalova K, Gachechiladze M, Narsia N, Bouchal J. The role of cancer-associated fibroblasts, solid stress and other microenvironmental factors in tumor progression and therapy resistance. *Cancer Cell Int*. 2014;**14**:41.
- 33 Fiorillo M, Peiris-Pages M, Sanchez-Alvarez R, Bartella L, Di Donna L, Dolce V, et al. Bergamot natural products eradicate cancer stem cells (CSCs) by targeting mevalonate, Rho-GDI-signalling and mitochondrial metabolism. *Biochim Biophys Acta Bioenerg*. 2018;**1859**:984–96.
- 34 Ginestier C, Monville F, Wicinski J, Cabaud O, Cervera N, Josselin E, et al. Mevalonate metabolism regulates Basal breast cancer stem cells and is a potential therapeutic target. *Stem Cells*. 2012;**30**:1327–37.
- 35 Eskiocak B, Ali A, White MA. The estrogen-related receptor alpha inverse agonist XCT 790 is a nanomolar mitochondrial uncoupler. *Biochemistry*. 2014;**53**:4839–46.
- 36 Whiteside TL. The tumor microenvironment and its role in promoting tumor growth. *Oncogene*. 2008;**27**:5904–12.
- 37 de Visser KE, Coussens LM. The inflammatory tumor microenvironment and its impact on cancer development. *Contrib Microbiol*. 2006;**13**:118–37.
- 38 Vitale I, Manic G, Coussens LM, Kroemer G, Galluzzi L. Macrophages and metabolism in the tumor microenvironment. *Cell Metab*. 2019;**30**:36–50.
- 39 Malekghasemi S, Majidi J, Baghbanzadeh A, Abdolalizadeh J, Baradaran B, Aghebati-Maleki L. Tumor-associated macrophages: protumoral macrophages in inflammatory tumor microenvironment. *Adv Pharm Bull*. 2020;**10**:556–65.
- 40 Wang J, Li D, Cang H, Guo B. Crosstalk between cancer and immune cells: Role of tumor-associated macrophages in the tumor microenvironment. *Cancer Med*. 2019;**8**:4709–21.
- 41 Gionfriddo G, Plastina P, Augimeri G, Catalano S, Giordano C, Barone I, et al. Modulating tumor-associated macrophage polarization by synthetic and natural PPARgamma ligands as a potential target in breast cancer. *Cell*. 2020;**9**:174.
- 42 Jablonski KA, Amici SA, Webb LM, Ruiz-Rosado Jde D, Popovich PG, Partida-Sanchez S, et al. Novel markers to delineate murine M1 and M2 macrophages. *PLoS ONE*. 2015;**10**:e0145342.
- 43 Ostuni R, Kratochvill F, Murray PJ, Natoli G. Macrophages and cancer: from mechanisms to therapeutic implications. *Trends Immunol*. 2015;**36**:229–39.
- 44 Patoli D, Mignotte F, Deckert V, Dusuel A, Dumont A, Rieu A, et al. Inhibition of mitophagy drives macrophage activation and antibacterial defense during sepsis. *J Clin Invest*. 2020;**130**:5858–74.
- 45 Wang Y, Li N, Zhang X, Horng T. Mitochondrial metabolism regulates macrophage biology. *J Biol Chem*. 2021;**297**:100904.
- 46 Costa A, Scholer-Dahirel A, Mechta-Grigoriou F. The role of reactive oxygen species and metabolism on cancer cells and their microenvironment. *Semin Cancer Biol*. 2014;**25**:23–32.
- 47 Xiang H, Ramil CP, Hai J, Zhang C, Wang H, Watkins AA, et al. Cancer-associated fibroblasts promote immunosuppression by inducing ROS-generating monocytic MDSCs in lung squamous cell carcinoma. *Cancer Immunol Res*. 2020;**8**:436–50.
- 48 Ippolito L, Morandi A, Taddei ML, Parri M, Comito G, Iscaro A, et al. Cancer-associated fibroblasts promote prostate cancer malignancy via metabolic rewiring and mitochondrial transfer. *Oncogene*. 2019;**38**:5339–55.
- 49 Maishi N, Hida K. Tumor endothelial cells accelerate tumor metastasis. *Cancer Sci*. 2017;**108**:1921–6.
- 50 De Bock K, Georgiadou M, Schoors S, Kuchnio A, Wong BW, Cantelmo AR, et al. Role of PFKFB3-driven glycolysis in vessel sprouting. *Cell*. 2013;**154**:651–63.
- 51 Draoui N, de Zeeuw P, Carmeliet P. Angiogenesis revisited from a metabolic perspective: role and therapeutic implications of endothelial cell metabolism. *Open Biol*. 2017;**7**:170219.
- 52 Eccles SA, Aboagye EO, Ali S, Anderson AS, Armes J, Berditchevski F, et al. Critical research gaps and translational priorities for the successful prevention and treatment of breast cancer. *Breast Cancer Res*. 2013;**15**:R92.
- 53 Raghav PK, Mann Z. Cancer stem cells targets and combined therapies to prevent cancer recurrence. *Life Sci*. 2021;**277**:119465.
- 54 Brabletz T, Kalluri R, Nieto MA, Weinberg RA. EMT in cancer. *Nat Rev Cancer*. 2018;**18**:128–34.
- 55 Singh A, Settleman J. EMT, cancer stem cells and drug resistance: an emerging axis of evil in the war on cancer. *Oncogene*. 2010;**29**:4741–51.
- 56 Ivaska J. Vimentin: central hub in EMT induction? *Small GTPases*. 2011;**2**:51–3.
- 57 Kokkinos MI, Wafai R, Wong MK, Newgreen DF, Thompson EW, Waltham M. Vimentin and epithelial-

- mesenchymal transition in human breast cancer – observations in vitro and in vivo. *Cells Tissues Organs*. 2007;**185**:191–203.
- 58 Loh CY, Chai JY, Tang TF, Wong WF, Sethi G, Shanmugam MK, et al. The E-cadherin and N-cadherin switch in epithelial-to-mesenchymal transition: signaling, therapeutic implications, and challenges. *Cell*. 2019;**8**:1118.
- 59 Onder TT, Gupta PB, Mani SA, Yang J, Lander ES, Weinberg RA. Loss of E-cadherin promotes metastasis via multiple downstream transcriptional pathways. *Cancer Res*. 2008;**68**:3645–54.
- 60 Chua HL, Bhat-Nakshatri P, Clare SE, Morimiya A, Badve S, Nakshatri H. NF-kappaB represses E-cadherin expression and enhances epithelial to mesenchymal transition of mammary epithelial cells: potential involvement of ZEB-1 and ZEB-2. *Oncogene*. 2007;**26**:711–24.
- 61 Feldker N, Ferrazzi F, Schuhwerk H, Widholz SA, Guenther K, Frisch I, et al. Genome-wide cooperation of EMT transcription factor ZEB1 with YAP and AP-1 in breast cancer. *EMBO J*. 2020;**39**:e103209.
- 62 Legrand C, Gilles C, Zahm JM, Polette M, Buisson AC, Kaplan H, et al. Airway epithelial cell migration dynamics. MMP-9 role in cell-extracellular matrix remodeling. *J Cell Biol*. 1999;**146**:517–29.
- 63 Fidler IJ, Poste G. The "seed and soil" hypothesis revisited. *Lancet Oncol*. 2008;**9**:808.
- 64 Quail DF, Joyce JA. Microenvironmental regulation of tumor progression and metastasis. *Nat Med*. 2013;**19**:1423–37.
- 65 Dias AS, Almeida CR, Helguero LA, Duarte IF. Metabolic crosstalk in the breast cancer microenvironment. *Eur J Cancer*. 2019;**121**:154–71.
- 66 Zhang QW, Liu L, Gong CY, Shi HS, Zeng YH, Wang XZ, et al. Prognostic significance of tumor-associated macrophages in solid tumor: a meta-analysis of the literature. *PLoS ONE*. 2012;**7**:e50946.
- 67 Arcucci A, Ruocco MR, Granato G, Sacco AM, Montagnani S. Cancer: an oxidative crosstalk between solid tumor cells and cancer associated fibroblasts. *Biomed Res Int*. 2016;**2016**:4502846.
- 68 Zhang Z, Gao Z, Rajthala S, Sapkota D, Dongre H, Parajuli H, et al. Metabolic reprogramming of normal oral fibroblasts correlated with increased glycolytic metabolism of oral squamous cell carcinoma and precedes their activation into carcinoma associated fibroblasts. *Cell Mol Life Sci*. 2020;**77**:1115–33.
- 69 Anderson NM, Simon MC. The tumor microenvironment. *Curr Biol*. 2020;**30**:R921–5.
- 70 Choi H, Moon A. Crosstalk between cancer cells and endothelial cells: implications for tumor progression and intervention. *Arch Pharm Res*. 2018;**41**:711–24.
- 71 Clendening JW, Pandya A, Boutros PC, El Ghamrasni S, Khosravi F, Trentin GA, et al. Dysregulation of the mevalonate pathway promotes transformation. *Proc Natl Acad Sci USA*. 2010;**107**:15051–6.
- 72 Mullen PJ, Yu R, Longo J, Archer MC, Penn LZ. The interplay between cell signalling and the mevalonate pathway in cancer. *Nat Rev Cancer*. 2016;**16**:718–31.
- 73 Swanson KM, Hohl RJ. Anti-cancer therapy: targeting the mevalonate pathway. *Curr Cancer Drug Targets*. 2006;**6**:15–37.
- 74 Gobel A, Breining D, Rauner M, Hofbauer LC, Rachner TD. Induction of 3-hydroxy-3-methylglutaryl-CoA reductase mediates statin resistance in breast cancer cells. *Cell Death Dis*. 2019;**10**:91.
- 75 Gazzo P, Proto MC, Gangemi G, Malfitano AM, Ciaglia E, Pisanti S, et al. Pharmacological actions of statins: a critical appraisal in the management of cancer. *Pharmacol Rev*. 2012;**64**:102–46.
- 76 Ahern TP, Lash TL, Damkier P, Christiansen PM, Cronin-Fenton DP. Statins and breast cancer prognosis: evidence and opportunities. *Lancet Oncol*. 2014;**15**:e461–8.
- 77 Osmak M. Statins and cancer: current and future prospects. *Cancer Lett*. 2012;**324**:1–12.
- 78 Bjarnadottir O, Romero Q, Bendahl PO, Jirstrom K, Ryden L, Loman N, et al. Targeting HMG-CoA reductase with statins in a window-of-opportunity breast cancer trial. *Breast Cancer Res Treat*. 2013;**138**:499–508.
- 79 Garwood ER, Kumar AS, Baehner FL, Moore DH, Au A, Hylton N, et al. Fluvastatin reduces proliferation and increases apoptosis in women with high grade breast cancer. *Breast Cancer Res Treat*. 2010;**119**:137–44.
- 80 Frattaruolo L, Carullo G, Brindisi M, Mazzotta S, Bellissimo L, Rago V, et al. Antioxidant and anti-inflammatory activities of flavanones from *Glycyrrhiza glabra* L.(licorice) leaf phytocomplexes: identification of licoflavanone as a modulator of NF-kB/MAPK pathway. *Antioxidants*. 2019;**8**:186.
- 81 Brindisi M, Frattaruolo L, Mancuso R, Palumbo Piccionello A, Ziccarelli I, Catto M, et al. Anticancer potential of novel α,β -unsaturated γ -lactam derivatives targeting the PI3K/AKT signaling pathway. *Biochem Pharmacol*. 2021;**190**:114659.
- 82 Iacopetta D, Lappano R, Cappello AR, Madeo M, De Francesco EM, Santoro A, et al. SLC37A1 gene expression is up-regulated by epidermal growth factor in breast cancer cells. *Breast Cancer Res Treat*. 2010;**122**:755–64.
- 83 Iacopetta D, Carrisi C, De Filippis G, Calcagnile VM, Cappello AR, Chimento A, et al. The biochemical properties of the mitochondrial thiamine pyrophosphate carrier from *Drosophila melanogaster*. *FEBS J*. 2010;**277**:1172–81.
- 84 Fiorillo M, Toth F, Brindisi M, Sotgia F, Lisanti MP. Deferiprone (DFP) targets cancer stem cell (CSC) propagation by inhibiting mitochondrial metabolism and inducing ROS production. *Cell*. 2020;**9**:1529.

Graphical Abstract

The contents of this page will be used as part of the graphical abstract of html only. It will not be published as part of main.



2 Direct activation of the ERR α pathway by high cholesterol levels promotes greater breast cancer aggressiveness with further activation of EMT process and pro-inflammatory cytokines release. Such effects drive greater macrophages infiltration with induction of an M2 phenotype, angiogenesis and endothelial branching, as well as a cancer-associated fibroblasts (CAFs) phenotype. These findings suggest the cholesterol-ERR α synergy as an interesting target for breast cancer treatment.